ATM AND AMPK REGULATE PEROXISOME DYNAMICS VIA PEX5 PHOSPHORYLATION IN RESPONSE TO STRESS

A Dissertation

by

JI JING

Submitted to the Office of Graduate and Professional Studies of
Texas A&M University
in partial fulfillment of the requirements for the degree of

DOCTOR OF PHILOSOPHY

Chair of Committee,	Yubin Zhou
Co-Chair of Committee,	Cheryl Walker
Committee Members,	Eric Jonasch
	Fen Wang
Head of Department,	Zimmer Warren

May 2018

Major Subject: Biomedical Sciences

ABSTRACT

Peroxisomes are single membrane-bound and autonomously replicating subcellular organelles. While their function as metabolic organelles is well known, their place in the world of cell signaling is only just beginning to emerge.

Peroxisomes are able to adjust their number in response to changing environmental and/or physiological conditions. It is crucial to maintain peroxisome homeostasis for normal cellular functions. High risk pathologies are associated with too few peroxisomes, such as peroxisome biogenesis disorders (PBDs), and too many peroxisomes, such as disorders that increase cellular ROS production to promote the development of disease, including cancer. Early studies have shown that pexophagy (selective autophagy of peroxisomes) is responsible for the decrease in superfluous or damaged peroxisomes, yet the mechanisms of initiation of pexophagy are not well defined, especially in mammalian cells. In Chapter II of this dissertation, we report a key role for the ataxia-telangiectasia mutated (ATM) kinase at the peroxisomes as a sensor of ROS that regulates pexophagy. ATM is recognized and localized to the peroxisome by PEX5. In response to ROS, ATM signaling activates ULK1 and suppresses mTORC1 to induce pexophagy. Concomitant with activation of ULK1, ATM phosphorylates PEX5 at Serine 141. This modification then promotes PEX5 mono-ubiquitination at Lysine 209. Mono-ubiquitinated PEX5 is

sufficient to target peroxisomes to the autophagosome via ubiquitin adaptor protein p62, leading to the initiation of pexophagy.

Peroxisomes do not contain DNA, hence all their proteins are encoded inside the nucleus, synthesized by free polyribosomes in the cytoplasm and delivered to peroxisome with the help of import receptors. It is known that PEX5 recognizes the peroxisome targeting sequence 1 (PTS1) of peroxisomal proteins and delivers them to peroxisome. However, how cells control this delivery has remained a mystery. In Chapter III of this dissertation, we found that AMP-activated protein kinase (AMPK) phosphorylates PEX5 at Ser279, which correlates with the import of peroxisomal proteins in response to low energy.

Thus, we have uncovered a previously unappreciated link between the peroxisome and the ATM and AMPK signaling pathways, which paves the way for a deeper understanding of peroxisome dynamics and its role in cellular metabolism.

DEDICATION

I would like to dedicate this dissertation to my family, and other loved ones, who inspire me.

To my mentor, Dr. Cheryl Lyn Walker, for her guidance and support. You have helped me throughout my doctoral training. If it weren't for you, I'm sure I wouldn't be who I am today.

To all my committee members, Dr. Yubin Zhou, Dr. Fen Wang and Dr. Eric Jonasch, for their support and kindness during my study.

To anyone who has shown me friendship and kindness during my life as a graduate student.

ACKNOWLEDGEMENTS

Appreciation and deepest gratitude goes to the following people who, in one way or another, have supported me and made this dissertation possible.

First of all, I would like to express the deepest appreciation and special thanks to my mentor, Dr. Cheryl Lyn Walker, for offering me this precious opportunity to undergo my Ph.D. training in USA; for her endless support; for her kind and understanding spirit; and for her guidance and help during my doctoral training. Dr. Cheryl Lyn Walker is also a great supervisor who guided me in preparing for public presentations, research paper writing, and early career development. She helped any time that I needed and provided direction toward completion of this project. The skills and knowledge which I have gained throughout my Ph.D. training are a very valuable component of my future career success. I also want to thank her for her kindness, help, and donation during Hurricane Harvey. I consider myself a very lucky individual, as I was provided with the opportunity of having her as my graduate advisor.

Secondly, let me express my sincere thanks and gratitude to my graduate advisor committee members: Dr. Yubin Zhou, Dr. Fen Wang and Dr. Eric Jonasch, who inspired me with millions of questions during my study. Dr. Yubin Zhou gave me the opportunity to conduct my research in his lab during my first rotation. He encouraged me during the whole training process and always offered me opportunities to participate in public presentations to improve my

communication skills. With his encouragement and support, I earned many great honors and awards. Dr. Fen Wang and Dr. Eric Jonasch gave me valuable advice on my project design and on how to better organize and present my research work. They were also very gracious with their time and helped me to perfect my writing and speaking skills to achieve a successful career in my future academic pursuits.

Thirdly, I am thankful to all members in Dr. Walker's lab. I am grateful for having a chance to meet so many wonderful people and professionals who helped me through my doctoral training. These experiments could not have been completed without the effort and co-operation from Dr. Durga Nand Tripathi and Dr. Jiangwei Zhang. We worked as a team and accomplished these projects together. Without their guidance and help, this dissertation would not have been possible. I also sincerely thank current lab members Dr. Ruhee Dere, Dr. Lindsey S. Trevino, Ms. Tia Berry, Dr. In Young Park, Dr. Tiffany A. Katz, Mr. Pratim Chowdhury, Ms. Rong He, Ms. Marijke Vanderhelm Schrock, Dr. Pavlos Msaouel, Mr. Riyad Navroz Seervai, Dr. Menuka Karki, and lab past members, Dr. Quan Wang, Dr. Lijun Liu, Dr. Elshad Hasanov and Dr. Xiande Liu for their generous support, coaching, and companionship during my graduate studies.

I am also sincerely thankful to all of the faculty, staff, and colleagues at the Texas A&M University Institute of Biosciences and Technology. In particular, I am grateful to Ms. Cynthia Lewis for solving all the administrative issues I met during my training and for pushing all the paperwork forward to ensure my

graduate studies proceeded smoothly. I would also like to thank Ms. Denelle Orellana, Miss. Dan Na Luo, Mr. Neeraj B Patel, and Ms. Eliria Mireles for helping to manage matters related to my training. Special thanks to Dr. Peter J.A. Davies and Kellie D. Garrett-Ekeland for giving me a hand during Hurricane Harvey. I am also thankful to Dr. Yun Nancy Huang for allowing me to finish my *in vitro* kinase assay under her protocol.

I would also like to express my deepest gratitude to all my friends. We have always stood by each other through the good times and the bad times. And finally, last, but by no means least, thanks to my parents for giving me encouragement, long-time support and unconditional love. Without them, I might not have completed my Ph.D. studies.

NOMENCLATURE

2-DG	2-Deoxy-D-Glucose
A	Alanine
ACC	Acetyl-CoA carboxylase
AMPK	AMP-activated protein kinase
AT	Ataxia telangiectasia
ATM	Ataxia-telangiectasia mutated
ATP	Adenosine triphosphate
Arg (R)	Arginine
BSA	Bovine Serum Albumin
CST	Cell Signaling Technology
Cys	Cysteine
DLP1	Dynamin-like protein 1
DMEM	Dulbecco's Modified Eagle Medium
DNA	Deoxyribonucleic Acid
ER	Endoplasmic reticulum
FBS	Fetal Bovine Serum
GAP	GTPase activating protein
GAPDH	Glyceraldehyde 3-Phosphate Dehydrogenase
H_2O_2	Hydrogen peroxide
HEK	Human embryonic kidney

HRP	Horseradish peroxidase
IR	Ionizing Radiation
KD	Kinase domain
LC3	Microtubule-associated protein 1 light chain 3
LCFAs	Long-chain fatty acids
LIR	LC3-interacting region
LKB1	Liver kinase B1
Lys (K)	Lysine
MEF	Mouse embryonic fibroblast
mTOR	Mammalian target of rapamycin
p62	SQSTM1 (Sequestosome 1)
PBS	Phosphate-buffered saline
PBDs	Peroxisome biogenesis eisorders
PD	Peroxisomal disorders
PEDs	Peroxisomal enzyme/transporter deficiencies
PEX	Peroxins
PMP	Peroxisome membrane protein
PTMs	Posttranslational modifications
PTS	Peroxisomal targeting signal
PVDF	Polyvinylidene difluoride
Q	Glutamine
Rheb	Ras homolog enriched in brain

RNA	Ribonucleic acid
RNS	Reactive nitrogen species
ROS	Reactive oxygen species
SDS-PAGE	SDS-polyacrylamide gels
Ser (S)	Serine
siRNA	short interfering ribonucleic acid
TBS-T	Tris-buffered saline with Tween-20
TCA	Tricarboxylic acid
TPR	Tetratricopeptide repeat
TSC	Tuberous sclerosis complex
UBA	Ubiquitin-associated domain
ULK1	Unc-51 like autophagy activating kinase
VLCFAs	Very-long-chain fatty acids
WT	Wild type
ZS	Zellweger syndrome

CONTRIBUTORS AND FUNDING SOURCES

Contributors

This work was supervised by a dissertation committee consisting of Professors Yubin Zhou (advisor) and Fen Wang of the Institute of Bioscience and Technology, Texas A&M University and Professor Cheryl Lyn Walker (co-advisor) of Baylor College of Medicine and Professor Eric Jonasch of MD Anderson Cancer Center.

Funding Sources

All work for Chapter II of the dissertation was completed by Ji Jing, in collaboration with Dr. Durga Nand Tripathi and Dr. Jiangwei Zhang. All the work for Chapter III of the dissertation was completed independently by Ji Jing.

This work was supported by the National Institutes of Health (NIH) Grant R01 CA143811 to Dr. Cheryl Lyn Walker. Ji Jing was a recipient of the Chinese scholarship Council fellowship.

TABLE OF CONTENTS

Page

LIST OF FIGURES

Page

LIST OF TABLES

Page

CHAPTER I

INTRODUCTION AND LITERATURE REVIEW

Peroxisomes are a class of small bodies enclosed by a single membrane found in the cytoplasm of all animal cells and many plant cells that range in size from 0.1 to 1.5µm[1]. Peroxisomes were first identified as “microbodies” using electron microscopy to analyze the cellular morphology of the mouse kidney in 1954[2]. Glyoxisomes are similar organelles, discovered in plant seeds in 1958, that oxidize stored lipids as a source of carbon and energy for growth[3]. At first, these two organelles were believed to be lysosomes because their morphology resembles that of lysosomes. However, in 1966, De Duve and Baudhuin were the first who isolated these “microbodies” from rat liver by cell-fractionation and discovered that the enzymes in these organelles differ greatly, in both composition and function, from those in lysosomes. They found that these microbodies were co-localized with production and detoxification oxidases of hydrogen peroxide (H_2O_2). Based on these findings, De Duve replaced the morphological name “microbodies” with the functional term “peroxisomes”[4].

Subsequent studies have shown that peroxisomes contain approximately 50 identified peroxisomal enzymes. These enzymes are involved in several key cellular metabolic pathways in eukaryotes, including β-oxidation of branched and very-long-chain fatty acids (VLCFAs) which results in the production of reactive oxygen species (ROS) as a byproduct of this enzymatic reaction. ROS are

chemically reactive species, including peroxides, superoxide, and hydroxyl oxygen.[5-7]. To combat the destructive effects of these molecules, peroxisomes also contain copious amounts of the enzyme catalase. When excess H_2O_2 accumulates in the cell, catalase decomposes H_2O_2 to H_2O:

$2\ H_2O_2 \xrightarrow{\text{Catalase}} 2H_2O + O_2$ (Figure 1. 1).

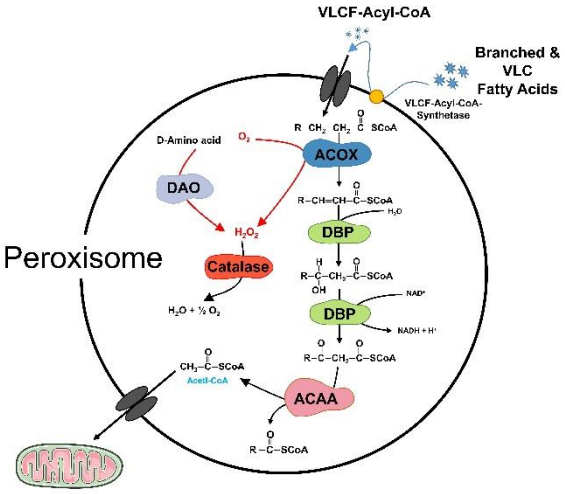

Figure 1. 1 Major metabolic pathways in peroxisomes.

It is now appreciated that peroxisomes have a much broader metabolic role than detoxification. For example, they catalyze the first two steps in the synthesis of plasmalogens. Furthermore, bile salts are also synthesized in peroxisomes. In plants, 2-phosphoglycolate, which is produced by the oxygenase action of rubisco in glyoxisomes[8,9]. In mammalian cells, mitochondria and peroxisomes are the two major sites of fatty acid β-oxidation. Both

organelles possess similar enzymes required for the degradation of fatty acids[10]. This is perhaps the best known example for peroxisome-mitochondria crosstalk. Very long- (>C26), long-chain (C22-C16) and branched fatty acids are major substrates for peroxisomal fatty acid β-oxidation. Peroxisomes oxidize these fatty acids down to a chain length of 6-8 carbon atoms, generating products such as acetyl-CoA and short-chain acyl-CoA that can subsequently be used for cytosolic fatty acid synthesis or exported to mitochondria for full degradation and generation of adenosine triphosphate (ATP) in the tricarboxylic acid (TCA)

Table 1. Sequences that target proteins from the cytosol to organelles.

Name	Location of Signal within Protein	Receptor	Nature of Signal
PTS1	C-terminus	PEX5	Tripeptide consensus S/A-L/R-L/M;
PTS2	N-terminus	PEX7 PEX5L	Nonapeptide with the sequence (R/K)-(L/V/I)-X_5-(H/Q)-(L/A)
PEX19-BS	--	PEX19	PEX19 Binding Sites

cycle[11]. One major difference between the two organelles is that mitochondrial β-oxidation is directly associated with the production of ATP whereas peroxisomal metabolism of fatty acid leads to the production of H_2O_2, but not ATP[12].

The process of peroxisome biogenesis consists three components: 1) peroxisome membrane formation, 2) peroxisomal proteins import, and 3) peroxisome division[13]. Peroxisomes do not contain their own genome. All peroxisomal proteins, both membrane and matrix, are encoded by nuclear genes and synthesized outside the organelle on “free” cytosolic ribosomes (ribosomes not bound to the rough endoplasmic reticulum)[14]. The newly made proteins are released into the cytosol and are then taken up by specific receptors into pre-existing peroxisomes. The targeting and import of membrane and matrix proteins to peroxisomes requires specific signal sequences, receptors, and translocation machineries. (Table 1.). For most peroxisomal proteins the uptake-targeting signal is known as peroxisomal targeting signal 1 (PTS1), which is located in the C-terminus consisting of a conserved tripeptide, usually with the sequence (S/A/C)-(K/R/H)-L[15,16]. Very few peroxisome matrix proteins contain an N-terminal PTS2, which is a nonapeptide with the sequence (R/K)-(L/V/I)-X5-(H/Q)-(L/A) (where X can be any amino acid)[17,18]. PTS1-or PTS2-containing matrix proteins are recognized by the soluble receptors: PEX5 (PTS1)[19] and PEX7 (PTS2)[18], and their co-receptors in the cytosol, which guide them to a docking site at the peroxisomal membrane. After translocation of the receptor-cargo complex to the luminal side of the peroxisomal membrane, the cargo is released and the receptors shuttle back to the cytosol[20]. PEX19 is an import receptor for peroxisomal membrane proteins with a PEX19 binding sites[21] (Figure 1. 2) and import usually membrane proteins of the peroxisomes. In

general, protein uptake into each of these organelles is an energy-requiring process that depends on integral proteins in the organelle membrane.

The growth and division of peroxisomes are not coupled to nuclear division. The organelles grow by the incorporation of proteins (and lipids), a process that occurs continuously during the interphase period of the cell cycle. There are two major mechanisms of peroxisomal biogenesis: 1) de novo pathway, and 2) the growth and fission pathway. The de novo peroxisomes are synthesized via budding from the endoplasmic reticulum (ER) to form the "mature peroxisome"[22]. The de novo pathway are including three steps: 1) incorporation of peroxisomal proteins into the ER membranes, 2) intra-ER sorting of peroxisomal proteins , and 3) vesicles fusion and peroxisome formation. Sec61 is essential for peroxisomal proteins imcorporation. Although peroxisomal fusion is not well defined, recent studies have indicated that some peroxisomal proteins (peroxin), such as PEX1 and PEX6 are necessary for fusion[23]. Another pathway of peroxisomal biogenesis is that PEX11 and Dynamin-like protein 1 (DLP1) mediates the membrane of pre-existing remodeling and elongation to initiate the fission and formation of new peroxisomes[24,25].

Mutations of peroxisomal proteins that cause defective peroxisome assembly occur naturally in the human population. These include disorders resulting from a defect in a single peroxisomal enzyme and disorders that result

from a deficiency in biogenesis of the peroxisome, referred to as peroxisome biogenesis disorders (PBDs) and peroxisomal enzyme/transporter

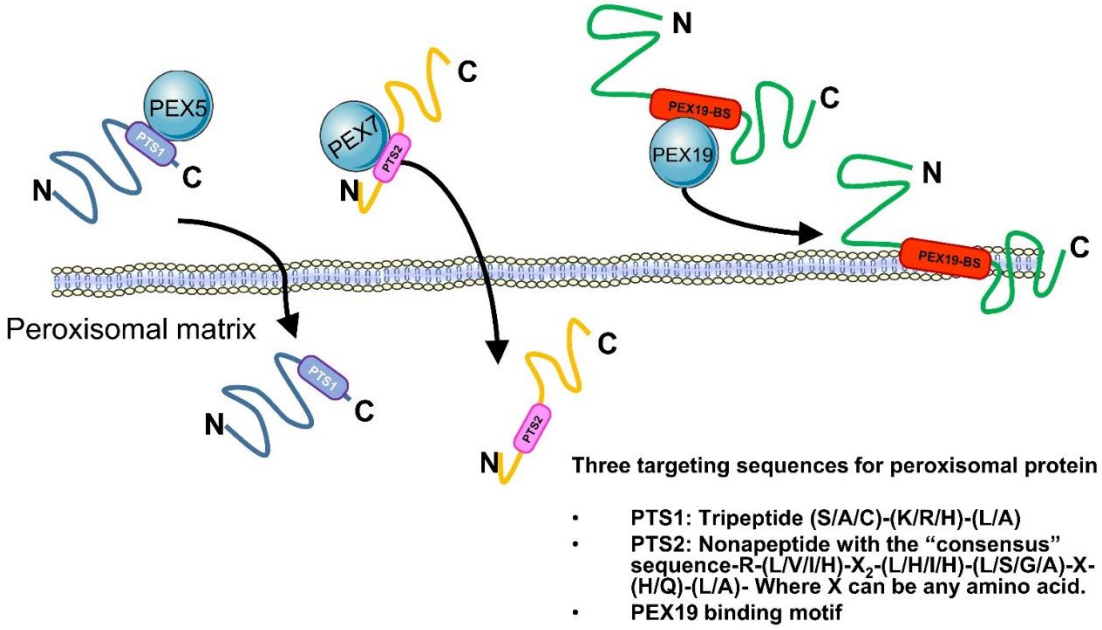

Figure 1. 2 Three targeting sequences for peroxisomal proteins.

deficiencies(PEDs)[26]. An example of PBDs is Zellweger Syndrome (ZS), which results in severe impairment of many organs and death. Patients with ZS are born with congenital neurological and other abnormalities and usually die within the first year of life[27]. In ZS and related disorders, the transport of all proteins into the peroxisomal matrix is impaired; newly synthesized peroxisomal enzymes remain in the cytosol and are eventually degraded. A remarkable feature of the ZS is that cells contain empty peroxisomes; these do contain a normal complement of peroxisomal membrane proteins. Several defects of peroxisomal

protein import, among them the PEX5-associated PTS1 pathway, have been found in such patients. In cell lines from Zellweger patients and from PEX5-knockout mice, peroxisomes are absent or grossly deficient and peroxisomal proteins are synthesized but remain localized to the cytoplasm and are subjected to degradation by proteolysis. These findings demonstrate that peroxisomes from patients with ZS are defective in the uptake of matrix proteins, but not of peroxisomal membrane proteins, from the cytosol. The ZS mutation causes a defect in a peroxisomal receptor or transport protein for peroxisomal matrix proteins but not membrane proteins. Recent studies have indicated that peroxisome function and dysfunction are associated with a wide variety of age-related maladies, including cancer, type 2 diabetes, and neurodegeneration.[5,28]

In mammalian cells, peroxisome proliferator-activated receptor α (PPAR α) mediates the induction of peroxisome proliferation[29]. The hyperactivation of PPAR α elevates peroxisome synthesis and basal β-oxidation rate, which causes more ROS generation. Induction of ROS at lower levels can activate cellular signaling pathways responsible for regulating cellular proliferation and survival, while high levels of ROS generation can lead to DNA damage directly, resulting in genomic instability and triggering the progression of cancer[30].

Thus peroxisomes are indispensable for human health and development. However, the mechanisms of regulation of peroxisomal homeostasis and matrix proteins transport have not been elucidated. This dissertation will 1) demonstrate ataxia-telangiectasia mutated (ATM) signaling and AMP-activated

protein kinase (AMPK) signaling at the peroxisome; 2) investigate the peroxisome as a new functional site for interaction of the ATM and the tuberous sclerosis complex (TSC) tumor suppressor to maintain peroxisomal homeostasis; and 3) identify AMPK phosphorylation of the PEX5 import receptor as a regulator of peroxisomal protein delivery.

CHAPTER II

ATM FUNCTIONS AT THE PEROXISOME TO INDUCE PEXOPHAGY IN RESPONSE TO ROS*

Introduction

Peroxisomes are autonomously replicating organelles.

Peroxisomes are autonomous, single membrane bound organelles that are involved in several key cellular functions in eukaryotic cells, including β-oxidation of branched and very-long-chain fatty acids. ROS, including H_2O_2, is a by-product of this enzymatic reaction[31,32]. While ROS can serve as signaling to molecule that mediate many normal cellular processes[33], excessive ROS can cause cellular damage, and trigger catabolic functions such as autophagy[34-36]. To prevent excessive production of ROS, cells must maintain peroxisome homeostasis by balancing peroxisome biogenesis with degradation[23,37-40]. Dysregulated peroxisome dynamics and dysfunctional peroxisomes have dramatic effects on human health and can give rise to many diseases. These diseases include ZS, PBDs [37,40,41], white matter disease[39] and Alzheimer's

---

* Part of this chapter is reprinted with permission from "ATM functions at the peroxisome to induce pexophagy in response to ROS" by Zhang, J[#]., Tripathi, D[#]., Jing, J[#]., Alexander, A., Kim, J., Powell, R., Dere, R., Tait-Mulder, J., Lee, J., Paull, T., Pandita, R., Charaka, V., Pandita, T., Kastam, M., and Walker, C, 2015, Nat Cell Biol. Oct;17(10):1259-1269. doi: 10.1038/ncb3230, Copyright [2015] by all authors. [#] These authors contributed equally to this work.

disease[38]. It is clear that maintaining peroxisome homeostasis is crucial for normal cellular metabolism, however, mechanisms for the initiation, recognition and turnover of excessive or dysfunctional peroxisomes to prevent pathologies are not well defined.

The major pathway of degradation for excess peroxisomes is autophagosomal-lysosomal fusion (pexophagy)[42-46]. Induction of pexophagy is initiated via target recognition by adapter proteins, such as the ubiquitin-binding autophagy adaptor p62/SQSTM1. p62/SQSTM1 has dual functions, it can interact with ubiquitinated target proteins via the C-terminal ubiquitin-associated (UBA) domain, and it can bind directly to microtubule-associated protein 1 light chain 3 (LC3) via LC3-interacting region (LIR) to link with the autophagy machinery [47]. Although other autophagy adaptor proteins have been identified, such as NBR1, and NDP52, only p62/SQSTM1has been shown to be involved in pexophagy [48,49]. There is a gap in our knowledge regarding how peroxisomal proteins are recognized by autophagy adapter(s), and which mechanisms are responsible for regulation of pexophagy.

The ATM and TSC Tumor Suppressors.

Ataxia telangiectasia mutated (ATM), the gene mutated in the cancer-prone human disease ataxia telangiectasia (AT), is a protein kinase that serves as a critical mediator of signaling pathways that facilitate the response of mammalian cells to ionizing radiation (IR) and other agents that induce

deoxyribonucleic acid (DNA) double-strand breaks [50]. Recent evidence suggests that ATM has the potential to function in a much broader number of protein networks than related to DNA damage[51] [52,53].

The tuberous sclerosis complex (TSC) is a tumor suppressor that functions as one of the gatekeepers for mammalian target of rapamycin complex 1 (mTORC1). The TSC signaling node is comprised of the GTPase activating protein (GAP) TSC2, its activation partner, TSC1, and its GAP target, the small GTPase Rheb [54,55]. The disease tuberous sclerosis results from defects in either the TSC1 or TSC2 tumor suppressor genes [56]. TSC2 participates in energy sensing and growth factor signaling to repress the kinase mTOR in the mTORC1 complex, a key regulator of protein synthesis and cell growth [57,58]. TSC inhibits the activity of the small GTPase-Rheb to repress mTORC1, which is a negative regulator of autophagy [45,59-63].

In previous studies, we have reported a novel function for ATM in the cytoplasm, where it activates TSC2 via the liver kinase B1 (LKB1)/AMPK metabolic pathway to repress mTORC1 signaling in response to ROS. We also have identified that the peroxisome is a signaling node involved in regulation of mTORC1 in response to ROS[64].

In this Chapter, we have continued this line of study and found that ATM binds to the peroxisome import receptor PEX5, and is localized and activated at peroxisomes. In response to ROS, it signals via AMPK and TSC to suppress mTORC1 and activate the autophagy initiating kinase ULK1, and PEX5 is

phosphorylated at Ser141 in an ATM-dependent manner, triggering its ubiquination at K209 and recognition by the autophagy adaptor protein p62 to induce pexophagy. These data are the first to demonstrate kinase signaling at the peroxisome, and point to a previously unappreciated role of ATM in an oxidative stress-signaling pathway important for inducing pexophagy to maintain peroxisome homeostasis.

Materials and Methods

Antibodies

Antibodies against lamin A/C (no. 2032, 1:1,000 WB), LC3B (no. 2775, 1:1,000 WB), HA (no. 3724, 1:2,000 WB), phospho-(S/T) ATM/ATR substrates (no. 2851, 1:1,000 WB) were purchased from Cell Signaling Technology. Phospho-ATM Ser 1981 (ab81292, 1:1,000 WB, 1:200 immunofluorescence (IF)), catalase (ab1877, 1:5,000 WB, 1:500 IF), HA (ab9110, 0.5 g per 100 g of total protein for immunoprecipitation (IP)), and PEX14 (ab109999, 1:1,000 WB) were purchased from Abcam. c-Myc (9E10; sc-40, 1:2,000 WB, 2 g per 100 g of total protein for IP), p62 (sc-28359, 1:1,000 WB), PEX1 (SC-21957, 1:500 WB), GAPDH (SC-25778, 1:5,000 WB), and PEX5 (SC-23188 1:300 IF) were purchased from Santa Cruz Biotechnology. Other antibodies used in this study are as follows: phospho-PEX5 (Ser 141) was generated by Covance, PEX5 (no. 12545-1-AP, 1:1,000 WB, 1:200 IF) were purchased from Proteintech. Flag (F3165, 1:4,000 WB, 1:500 IF, 1.25 g per 100 g of total protein for IP), PMP70 (SAB4200181, 1:5,000WB, 1:500 IF) and ubiquitin (U5379, 1:100 IF) were purchased from Sigma. ATM (GTX70103, 1:1,000) was from GeneTex; LDH (AB1222, 1:2,000 WB) was from Chemicon; β-integrin (no. 610468, 1:2,000 WB) was from BD Transduction Laboratories; p62 (03-GP62-C, 1:100) was from ARP. Secondary antibodies conjugated to horseradish peroxidase were purchased from Santa Cruz Biotechnology. Secondary antibodies for

immunofluorescence staining were obtained from Molecular Probes. Reagents are as follows: hydrogen peroxide solution (323381-25ML) was purchased from Sigma. Ku55955 was obtained from Tocris Bioscience.

Cell culture and transfection

Wild-type (WT) (GM15871) fibroblast cells, WT human fibroblast (GM08399) and ataxia-telangiectasia (AT) patients fibroblast (GM05849) cells were purchased from Coriell Cell Repositories and cultured in MEM supplemented with 15% fetal bovine serum (FBS). HEK293 (ATCC) cells were cultured in DMEM supplemented with 10% FBS. HepG2 (ATCC) cells were cultured in MEM supplemented with 10% FBS. FAO (Sigma) cells were cultured in F12 media supplemented with 10% FBS and 2mM L-glutamine (Life technologies). MCF7 cells were grown in modified IMEM media supplemented with 10% FBS. All media and FBS were purchased from Life Technologies and Sigma respectively. Indicated DNA transfections were performed using the Lipofectamine 2000 reagent (Invitrogen) according to the manufacturer's instructions. All of the cell lines were tested and confirmed negative for mycoplasma.

Plasmids and mutagenesis

We used EST cDNA clone (Expressed-sequence tags, GE Healthcare) as a template to get the full-length hPEX5 by PCR. hPEX5 PCR product was

cloned into pJET1.2/blunt cloning vector to amplify full-length hPEX5 with SalI restriction sites. pCMV-Myc-PEX5 was made by inserting amplified fragments, with SalI restriction sites. Mutagenesis of pCMV-Myc-PEX5 was performed by the QuikChange LightningMulti Site-Directed Mutagenesis Kit. The primers for different sites were designed as follows (Table 2).

RNAi knockdown

Endogenous gene in cells were knocked down with 20nM siRNA each designed for targeting ATM, PEX5, p62/SQSTM1, and PEX2/10/12. siRNA is purchased from Dharmacon. The siRNA information for different genes is followed: On-TARGETplus ATM siRNA (L-003201-00-0005), SiGENOME human PEX2, PEX10 and PEX12 siRNA (M-006548-02, M-006545-00, and M-019337-02), si SMARTpool human PEX5 (M-015788-00) and si SMARTpool human SQSTM1 (M-010230-00). HEK293 cells were transfected with the indicated siRNA at 20nM final concentrations with DharmaFECT 1 (GE Dharmacon) according to the manufacturer's instructions for 72 h before collection of lysates. As a transfection control, we used an equal amount of control siRNA.

Cellular fractionation

Wash and collect cells, pellet at 1500 rpm for 5min at 4℃ for twice. Resuspend the pellet in 5 volumes of hypotonic buffer containing complete protease inhibitor (10 mM HEPES, pH 7.2, 10 mM KCl, 1.5 mM $MgCl_2$, 0.1 mM

EGTA, 20 mM NaF, and 100 μM Na_3VO_4). Break cells to release nuclei a Dounce homogenizer for 50-100 times depending on cell type. Centrifuge Dounced cells at 3,000 rpm at 4℃ for 5 min to pellet crude nuclei and other fragments and get supernatant A. Crude nuclei (pellet A) were resuspended with hypotonic buffer containing complete protease inhibitor and homogenized using a Dounce homogenizer. Discard the supernatant by centrifugation at 3000 rpm for 5 min at 4℃. Wash the pellet with nuclear wash buffer (10 mM Tris-HCl, pH 7.4, 0.1% NP-40, 0.05% Na-Deoxycholate, 10 mM NaCl, and 3 mM $MgCl_2$). Then the pellet (nuclear fraction) was lysed in high salt lysis buffer (20 mM HEPES, pH 7.4, 0.5 M NaCl, 0.5% NP-40, and 1.5 mM $MgCl_2$). The supernatant A can be retained as the cytoplasmic fraction. The supernatant A separated by ultracentrifugation at 29,000 rpm for 1 h at 4℃. Collect the supernatant B, or cytosolic fraction. The pellet B (membrane containing fraction) was lysed in 1× CST lysis buffer (as above) containing complete protease inhibitor. Remove the insoluble fractions by centrifugation at max speed for 10 min at 4 ℃, then get membrane lysate.

Peroxisome Isolation

Peroxisome isolation was performed using the Peroxisome Isolation Kit (Sigma) according to the manufacturer's protocol. Briefly, cells were washed by scraping into ice-cold phosphate-buffered saline (PBS) to remove the serum. Pellet cells at 1,200 rpm for 5min at 4℃ and discard the supernatant for twice.

The cells were resuspended in 2.7 times packed cell volum 1×Peroxisome Extraction Buffer, homogenized the cells in Dounce homogenizer, and centrifuged at 1,000 g for 10 minutes. Transfer the supernatant to a new centrifuge tube and centrifuge at 2,000 g for 10 minutes. Collect the supernatant and further centrifuge at 25,000 g for 20 minutes. Resuspend the pellet in a minimal volume of 1×Peroxisome Extraction Buffer, and subjected to density gradient centrifugation at 100,000 g for 1.5 hours. The purified peroxisomes were enriched in the bottom layer of the density gradient.

Western blot and Immunoprecipitation assay

The cells were lysed directly with Cell Signaling Technology (CST) lysis buffer (20mM Tris-HCl (pH 7.5), 150mM NaCl, 1mM EDTA, 1mM EGTA, 1% Triton X-100, 2.5mM Na pyrophosphate, 1mM β-glycerophosphate, and 1× protease inhibitor cocktail and phosphatase inhibitor cocktail 2 and 3), and rotated for 30 min at 4 ℃. Lysates were microcentrifuged at 4 ℃.at maximum speed (10,000g) for 10 min. The supernatant was subjected to BCA Protein Assay (Thermo Scientific) to quantify protein levels. For immunoprecipitation, the indicated antibody was coupled with Magnetic protein A/G beads (Thermo Scientific) and incubated with cell lysates overnight at 4 ℃.The beads were washed with lysis buffer 5 times before being resolving by SDS-PAGE. The cell lysates were separated on a 4-15% gel (Bio-Rad), transferred to PVDF membranes and probed with indicated antibodies. Quantification of expression

levels was performed using ImageQuantTL software and data were normalized with GAPDH expression. Student's t-test (two-tailed) was performed on at least three biological repeats using GraphPad Prism software. Error bars represent standard deviations of normalized fold changes.

Protease protection assay

The crude peroxisomal fraction was isolated using the Peroxisome Isolation Kit (Sigma). The fractionation sample was incubated with Proteinase K (Roche) 0.1 μg ml^{-1} with or without 1% Triton X-100 on ice for 5, 15 and 30 min respectively. The reaction was stopped by phenylmethyl sulphonyl fluoride and samples were processed by western blot assay.

Immunofluorescence microscopy

Seed cells on coverslips and culture at 37℃ and 5% CO_2 for 24 h before staining. Cells were washed with 1×PBS three times and fixed for 15 min in 4% paraformaldehyde, permeabilized for 10 min in 0.5% Triton X-100 in PBS and blocked with 3.75% BSA in PBS for 1 h at room temperature. Then the cells were stained with the indicated primary antibody overnight at 4 ℃. Secondary antibodies were incubated for 1 h at 37 ℃. Nuclei were counterstained with DAPI for 2 min. Slides were mounted using SlowFade Gold Antifade reagent (Life Technologies). Images were captured using either a Deltavision Deconvolution Microscope (DeltaVision Elite, GE) or a Nikon confocal system.

Images were acquired with a × 60/1.42 oil objective (Olympus). SoftWoRx software was used for acquisition of image stacks, time-lapse and deconvolution. For time-lapse, the cells were seeded on glass-bottom micro-well dishes (MatTek) for 24 h ahead of time and then immediately treated with H_2O_2 before image acquisition on the stage. Images were quantified using ImageJ software. All confocal images are representative of 4 independent experiments were used for quantification.

RNA extraction and Quantitative real-time polymerase chain reaction (qPCR)

Total RNA was isolated using the RiboPure Kit (Life technologies), and the first strand cDNA was generated from total RNA using oligo-dT primers and reverse transcriptase II (Life Technologies). Briefly, cells were plated in 6-well plates and cultured at 37 ℃ and 5% CO_2 for 24 h ahead of treating cells with indicated condition. The cells were washed with PBS three times before scraping in 1 ml TRI Reagent solution (Ambion). One millilitre of the homogenate was transferred to a 1.5ml centrifuge tube. Two hundred microlitres of chloroform was added and vortexed at maximum speed. Following a 5 min incubation at room temperature, the samples were centrifuged at maximum speed for 10 min. Four hundred microlitres of the aqueous phase was transferred to a new tube followed by addition of 200 µl 100% ethanol. The sample was transferred to a Filter Cartridge-Collection and centrifuged 1 min at maximum speed. The column was washed with 70% ethanol and 100 µl of

elution buffer was added to elute RNA. qPCR was performed with the Taq Man Fast Universal Kit and the ABI Viia7 analyzer (Applied Biosystems). Target gene expression values were normalized to human *GAPDH*. The primers were purchased from Life Technologies.

Statistical analysis

The data are shown as mean ± s.d. Student's t-test (two-tailed) was performed for the comparisons between two groups and $P < 0.05$ was considered statistically significant. All experiments were repeated at least three times and representative data are shown as indicated.

Table 2. Primers for plasmid construction and mutagenesis

Gene Name		Sequence (from 5'-3')
hPEX5	Forward	CGGTCGACCATGGCAATGCGGGAG
	Reverse	GTCGACTCACTGGGGCAGGCCAAAC
hPex5-S141A	Forward	GAGACTGACTGGGCCCAAGAATTCATC
	Reverse	GATGAATTCTTGGGCCCAGTCAGTCTC
hPex5-S141E	Forward	CGGTCGACCATGGCAATGCGGGAG
	Reverse	GTCGACTCACTGGGGCAGGCCAAAC
hPex5-S279A	Forward	GTTTGAACGAGCCAAGGCAGCTATAGAGTTGCAG
	Reverse	CTGCAACTCTATAGCTGCCTTGGCTCGTTCAAAC
hPex5-S621A	Forward	GACGCGCGGGATCTGGCCACCCTCCTAACTATG
	Reverse	CATAGTTAGGAGGGTGGCCAGATCCCGCGCGTC
hPex5-K28R	Forward	CCCAGGACAGGGCCCTTCG
	Reverse	CGAAGGGCCCTGTCCTGGG
hPex5-K52R	Forward	GGCAGCCTCCAGGCCTTTGGGAG
	Reverse	CTCCCAAAGGCCTGGAGGCTGCC
hPex5-K170R	Forward	CAATCAGAGGAGAGGCTGTGGCTGGGAG
	Reverse	CTCCCAGCCACAGCCTCTCCTCTGATTG
hPex5-K204R	Forward	CTTTGTGGCCAGAGTGGATGAC
	Reverse	GTCATCCACTCTGGCCACAAAG
hPex5-K209R	Forward	GATGACCCCAGATTGGCTAATTC
	Reverse	GAATTAGCCAATCTGGGGTCATC
hPex5-K292R	Forward	GAGGAGATGGCAAGACGGGATGCTGAG
	Reverse	CTCAGCATCCCGTCTTGCCATCTCCTC
ATM R3047Q	Forward	GACCCCAAAAATCTCAGCCAACTTTTCCCAGGATGGAAAGC
	Reverse	GCTTTCCATCCTGGGAAAAGTTGGCTGAGATTTTTGGGGTC

Results

ATM kinase localizes to the cytosolic surface of peroxisomes

To investigate the subcellular localization of ATM, HEK293 cells were fractionated, revealing that endogenous ATM was detected in the nuclear (lamin A/C containing), in the membrane (β-integrin containing) and in the peroxisome (PMP70 and catalase containing) fractions (Figure 2. 1A) but not within the cytosolic fraction. This is consistent with previous reports that ATM is a DNA damage response sensor in the nucleus[50,65] that localizes to the membrane and to peroxiomes [66,67]. The localization of ATM within the peroxisomal membrane or matrix was further determined by protease protection assay. Isolated peroxisomes were treated with proteinase K in the absence or presence of membrane disrupting detergent TritonX-100 *in vitro*. The peroxisomal membrane protein PMP70 and ATM were degraded in both absence and presence of TritonX-100, while catalase, peroxisome matrix protein, was resistant to proteinase K (Figure 2. 1B), indicating that ATM was associated with the outer surface of peroxisomal membranes.

ATM is activated at the peroxisome in response to ROS.

Previous studies have shown that ATM has a cytoplasmic function and participates in the cellular response to ROS damage. ROS-induced ATM activation regulates mTORC1 signaling and autophagy via the

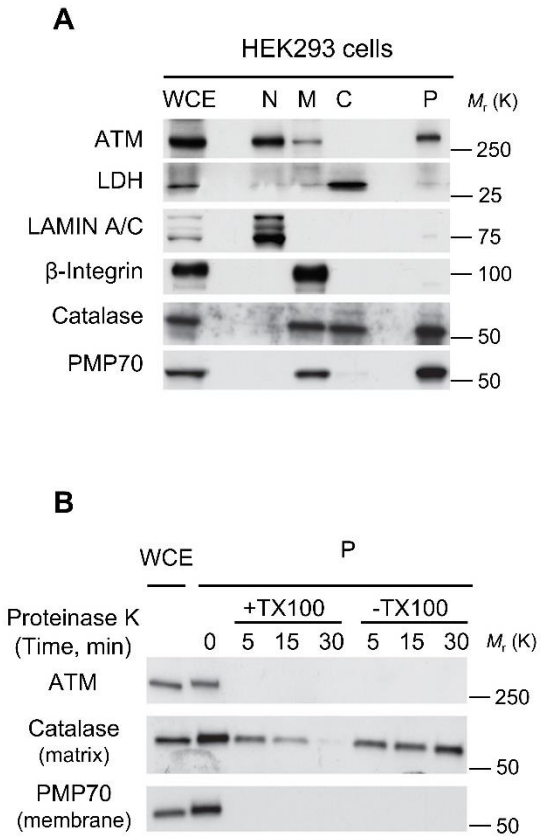

Figure 2. 1 ATM is a peroxisome-localized kinase.

A. Subcellular fractionation of HEK293 cells demonstrating the localization of ATM. Catalase and PMP70 were used as subcellular markers of peroxisomal matrix and membrane proteins (P), respectively. LDH, lamin A/C and β-integrin were used as markers for cytosolic (C), nuclear (N) and membrane (M) fractions, respectively. WCE, whole-cell extract. **B.** Proteinase K assay in the presence or absence of Triton X-100 performed with peroxisomal fractions obtained from HEK293 cells. Immunoblotting was performed with ATM, catalase and PMP70 antibodies. WCE, whole-cell extract; P, peroxisome fraction.

LKB1/AMPK/TSC2 signaling node[53]. To investigate whether peroxisome-localized ATM was activated in response to ROS, we purified peroxisomes from cells exposed to H_2O_2 and observed an increase in activated ATM in the peroxisome fraction (increased immunoreactivity with a phospho-specific ATM (S1981) antibody) (Figure 2. 2A). Localization of endogenous phospho-ATM to peroxisomes was confirmed by deconvolution microscopy, which demonstrated that co-localization of phospho-ATM with the peroxisomal protein catalase was increased in human fibroblasts in the presence of H_2O_2 (Figure 2. 2B). Together, these data identify the peroxisome as a site for activation of ATM in the cytoplasm in response to ROS.

PEX5 localizes ATM to the peroxisome

Most peroxisomal proteins contain a PTS1 motif, which is recognized by soluble receptors PEX5[68]. Previous studies have been shown that ATM containes a putative PEX5 binding sequence (SRL) at its C-terminus[67] (Figure 2. 3A). Interestingly, we found that endogenous ATM could be co-immunoprecipitated with PEX5, and the interaction between activated ATM (phospho-ATM) and PEX5 was increased by H_2O_2. (Figure 2. 3B). To test whether the putative PEX5 binding sequence-SRL was required for ATM interaction with PEX5 and localization of ATM to the peroxisome, we introduced an arginine (R) to glutamine (Q) mutation into wild-type ATM at amino acid position 3047 (R3047Q). Localization of the ATM R3047Q mutant in the

peroxisome fraction was dramatically decreased (Figure 2. 3C), because the mutant disturbed the interaction between ATM and PEX5 (Figure 2. 3D). These data were confirmed by immunocytochemistry, where ATM-WT was significantly increased and co-localized with the peroxisome membrane protein PMP70 in the cytoplasm in response to ROS. In contrast, the ATM-R3047Q mutant remained primarily nuclear, and exhibited little co-localization with PMP70 by H_2O_2 (Figure 2. 3E). These results indicate that ATM is localized to the peroxisome by PEX5.

PEX5 is a substrate of ATM

The increased interaction of phospho-ATM with PEX5 in the presence of ROS (Figure 2. 3B) suggested that PEX5 might also be a target for the ATM kinase. Immunoprecipitated PEX5 was recognized by a pan-phospho-(S/T) ATM substrate antibody, and immunoreactivity was significantly increased by H_2O_2 treatment (Figure 2. 4A). The immunoreactivity of PEX5 with the pan-phospho-(S/T) ATM substrate antibody was abrogated by the ATM inhibitor KU55933. Furthermore, PEX5 immunoreactivity to the ATM substrate antibody was lost in AT fibroblasts, which lack ATM (Figure 2. 4B). These data demonstrate that PEX5 is a target for ATM.

ATM phosphorylates PEX5 at Ser141 in response to ROS.

ATM is a highly selective kinase that prefers substrates with S*/T*Q motif hydrophobic residues in the N-1 and the N-3 positions and negatively charged

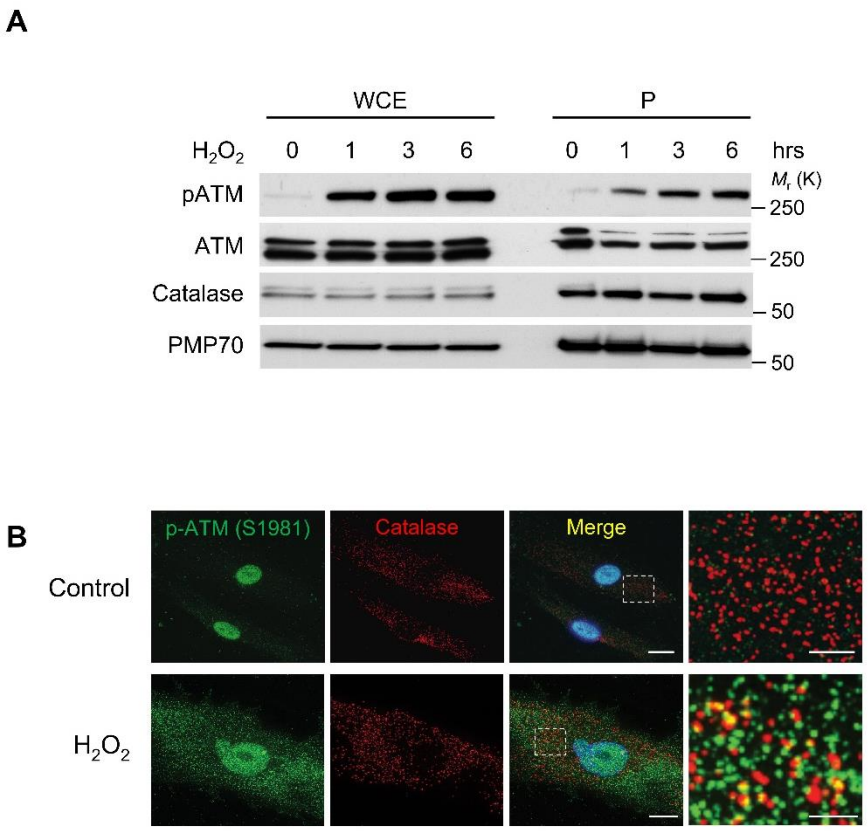

Figure 2. 2 ATM is activated at peroxisome in response to ROS.

A. HepG2 cells treated with H_2O_2 (0.4 mM) at 1, 3, 6 h. Whole cell extracts (WCE) and peroxisomal fractions (P) were probed with the indicated antibodies. **B.** Representative images of wild-type (GM15871) fibroblasts treated with or without H_2O_2 for 1 h and immunostained for active pATM (Ser 1981; green) and catalase (red). Scale bars, 15 μm. The insets show the regions outlined by dashed lines at higher magnification. Scale bar, 5 μm.

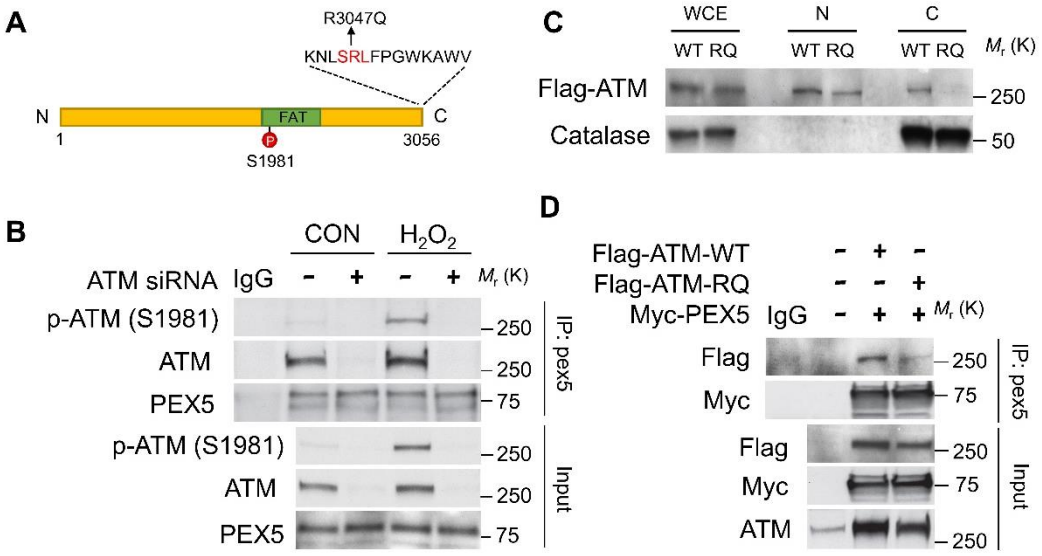

Figure 2. 3 ATM is localized to the peroxisome by PEX5.

A. Schematic indicating the putative PEX5-binding region-SRL sequence at the C-terminus of ATM. **B.** Co-immunoprecipitation with anti-PEX5 antibody in HepG2 cells transfected with control or ATM siRNA and treated with H_2O_2 (0.4 mM) for 3 h followed by immunoblotting with the indicated antibodies. **C.** Subcellular fractionation of HEK293 cells overexpressing Flag–ATM-WT or Flag–ATM-RQ (mutant). Immunoblotting was performed with the indicated antibodies. WCE, whole-cell extract; N, nuclear; P,peroxisome fraction. **D.** Immunoprecipitation was performed with anti-Myc antibody in HEK293 cells overexpressing Myc–PEX5 with Flag–ATM-WT or Flag–ATM-RQ and immunoblotted with Flag. Inputs were immunoblotted using the indicated antibodies. **E.** Representative images of HEK293 cells overexpressing Flag–ATM-WT and treated with or without H_2O_2 (0.4 mM) for 1 h and immunostained for Flag (ATM-green) and PMP70 (peroxisome-red). Scale bars, 10μm. High-magnification images of the outlined areas are shown to the right. Scale bars, 5μm. The plot on the right shows the quantification of ATM and PMP70 co-localization.

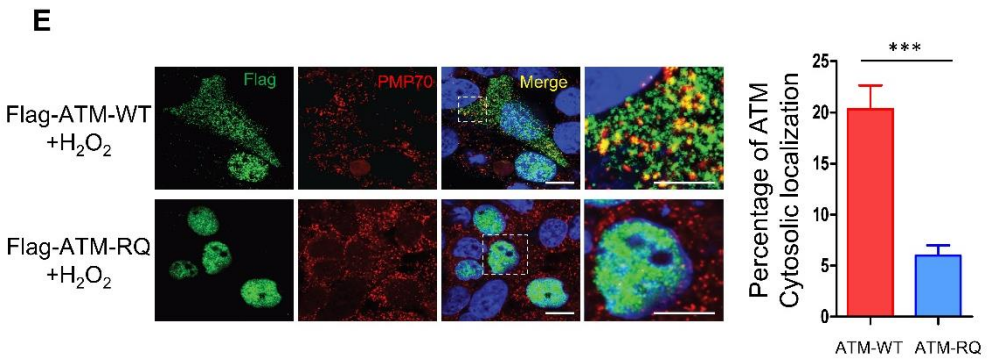

Figure 2. 3 Continued.

residue at N+1 position[69]. Moreover, *in silico* analysis using the Scansite program (http://scansite.mit.edu/) identified a potential ATM phosphorylation site in PEX5 at Ser 141 (Figure 2. 5A). Ser 141 is highly conserved in PEX5 in multiple species and is similar to other ATM substrates, such as p53, CHK2, and BRCA1 (Figure 2. 5B). Serine has a nucleophilic (–OH) group that attacks of the γ-phosphate group (γ-PO_3^{2-}) on the universal phosphoryl donor adenosine triphosphate (ATP), resulting in the transfer of the phosphate group to the Serine[70,71]. However, alanine does not contain –OH group, mutating serine to alanine effectively prevents potential serine phosphorylation. To determine if loss of Ser141 abrogated ATM phosphorylation of PEX5 serine 141 of PEX5 was mutated to alanine (S141A). In PEX5-WT, immunoreactivity with the pan-phospho-(S/T) ATM substrate antibody increased with H_2O_2 treatment, while the S141A PEX5 mutant was not recognized by the pan-phospho-(S/T) ATM substrate antibody (Figure 2. 5C). We next generated a polyclonal antibody

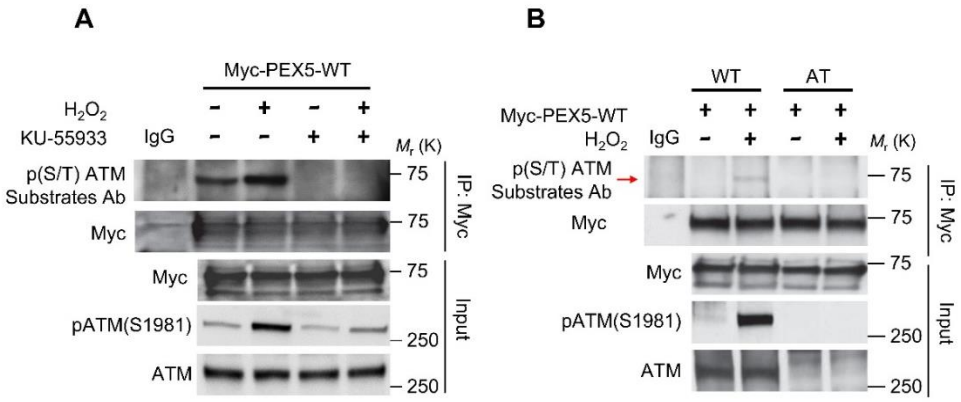

Figure 2. 4 PEX5 is a substrate of ATM.

A. Immunoprecipitation performed with anti-Myc antibody of lysates from HEK293 cells overexpressing Myc–PEX5, treated with H_2O_2 (0.4 mM) for 1 h in the presence/absence of an ATM inhibitor (KU-55933, 2 h pretreatment) followed by immunoblotting with phospho-(S/T) ATM substrate antibody. Inputs were immunoblotted using the indicated antibodies. **B**. WT fibroblasts (GM08399) and AT fibroblasts (GM05849) were transfected with Myc-PEX5-WT and treated with H_2O_2 for 1 h. The complex was immunoprecipitated with anti-Myc and immunoblotted with phospho-(S/T) ATM substrate antibody. Inputs were immunoblotted using the indicated antibodies.

against the phospho-Ser 141 of PEX5 and confirmed that phosphorylation of PEX5-WT at Ser 141 was increased, but not S141A mutant PEX5 in response to ROS (Figure 2. 5D). The increased phosphorylation at Ser 141 of PEX5 in response to ROS was lost with siRNA knockdown of ATM (Figure 2. 5E). Together, these data demonstrate that PEX5 is phosphorylated on Ser 141 in response to ROS, and that this phosphorylation is ATM-dependent.

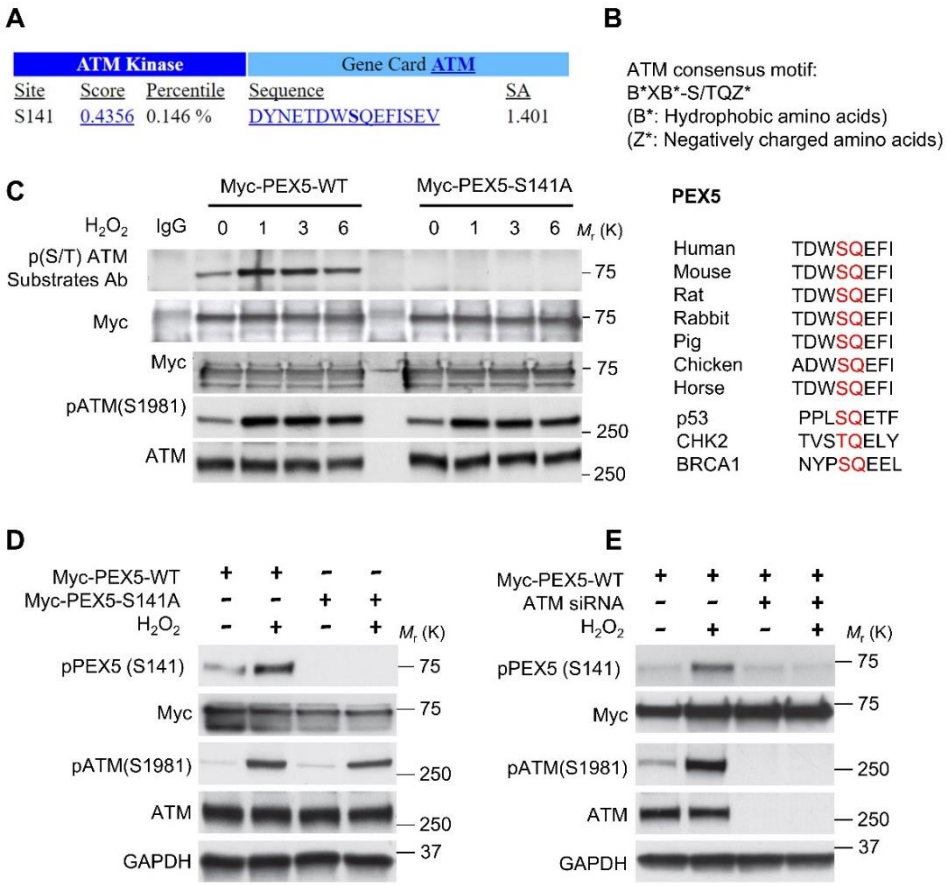

Figure 2. 5 ATM phosphorylates PEX5 at Ser 141 in response to ROS.

A. Prediction of PEX5 phosphorylation site and ubiquination site by ScanSite. **B.** Conserved S141 (ATM phosphorylation site) sequence in PEX5. **C.** HEK293 cells transfected with either a Myc–PEX5-WT or Myc–PEX5-S141A mutant construct treated with H_2O_2 (0.4 mM) for the indicated times. Immunoprecipitation was performed with an anti-Myc antibody followed by immunoblotting with phospho-(S/T) ATM substrate antibody. **D.** HEK293 cells transfected with either a Myc–PEX5-WT or Myc–PEX5-S141A mutant construct treated with H_2O_2 (0.4 mM) for 1 h. Western analysis was performed with the indicated antibodies. **E.** HEK293 cells transfected with Myc–PEX5-WT for 24 h following a siRNA knockdown of ATM for 48 h treated with H_2O_2 (0.4 mM) for 1 h. Western analysis was performed with indicated antibodies.

PEX5 is mono-ubiquitinated in response to ROS.

Selective autophagy of peroxisomes is considered a major pathway for peroxisome degradation[46]. Ubiquitin is a key degradation signal, which is involved in selective autophagy of misfolded proteins or damaged organelles[72]. Although ubiquitin on the peroxisome membrane surface is thought to target peroxisomes to the autophagosome for degradation[49], the initiation and specific site(s) of ubiquitination for peroxisomal degradation have not been investigated. As membrane-bound PEX5 has been reported to be ubiquitinated, becoming either poly-ubiquitinated and targeted for proteasome-mediated degradation, or mono- ubiquitinated for recycling back to the cytosol[73-77], we determined whether PEX5 is ubiquitinated in response to ROS. Myc-PEX5 and HA-Ub were co-transfected in HEK293 cells. Co-immunoprecipitation assays showed that immunoreactivity to a Myc antibody (an indicator of ubiquitinated PEX5) was significantly increased by ROS (Figure 2. 6A). It is possible that PEX5 is mono-ubiquitinated, as we observed one specific band. To confirm that PEX5 is indeed mono-ubiquitiylated in response to ROS, HA-Ub-K0 (ubiquitin with all lysine residues mutated to arginine to prevent chain formation and poly-ubiquitination) was co-expressed with Myc-PEX5 in HEK293 cells. There was no observed decrease in the apparent molecular weight, or amount of PEX5 ubiquitination in response to ROS using the HA-Ub-K0 construct (that can only be mono-ubiquitinated), compared to the HA-Ub-WT construct (Figure 2. 6B), indicating PEX5 was mono-ubiquitinated in response to ROS.

PEX2, PEX10 and PEX12 are E3 ligases for PEX5 ubiquitination

Three RING peroxisome biogenesis factors (peroxins) PEX2, PEX10, and PEX12 have been identified as part of a peroxisome-localized E3 ligase responsible for poly-ubiquitination of PEX5[76,78]. To identify E3 ligase of PEX5 mono-ubiquitination in response to ROS. We knocked down PEX2, PEX10, and PEX12 with short interfering RNA (siRNA), and found that siRNA knockdown of these peroxins reduced ubiquitination of PEX5 in response to ROS (Figure 2. 7A-B), indicating that PEX2, PEX10, and PEX12 are E3 ligases for PEX5 mono-ubiquitination.

PEX5 is mono-ubiquitinated at Lys 209

The putative ubiquitination sites on PEX5 were identified using PhosphoSite (www.phophosite.org). Using site-directed mutagenesis, we introduced a series of Lysine (K) to Arginine (R) mutation constructs. We observed that, compared to other lysines in PEX5, mutation of lysine 209 dramatically decreased PEX5 ubiquitination (Figure 2. 8). Lysine 209 was further supported as a *bona fide* site for PEX5 ubiquitination by publically available mass spectrometry databases (www.phosphosite.org)[79].

ROS-induced PEX5 ubiquitination is ATM-dependent

Phosphorylation can regulate ubiquitination of a protein by promoting recognition by an E3 ligase and creating a phosphodegron [80]. Therefore, we

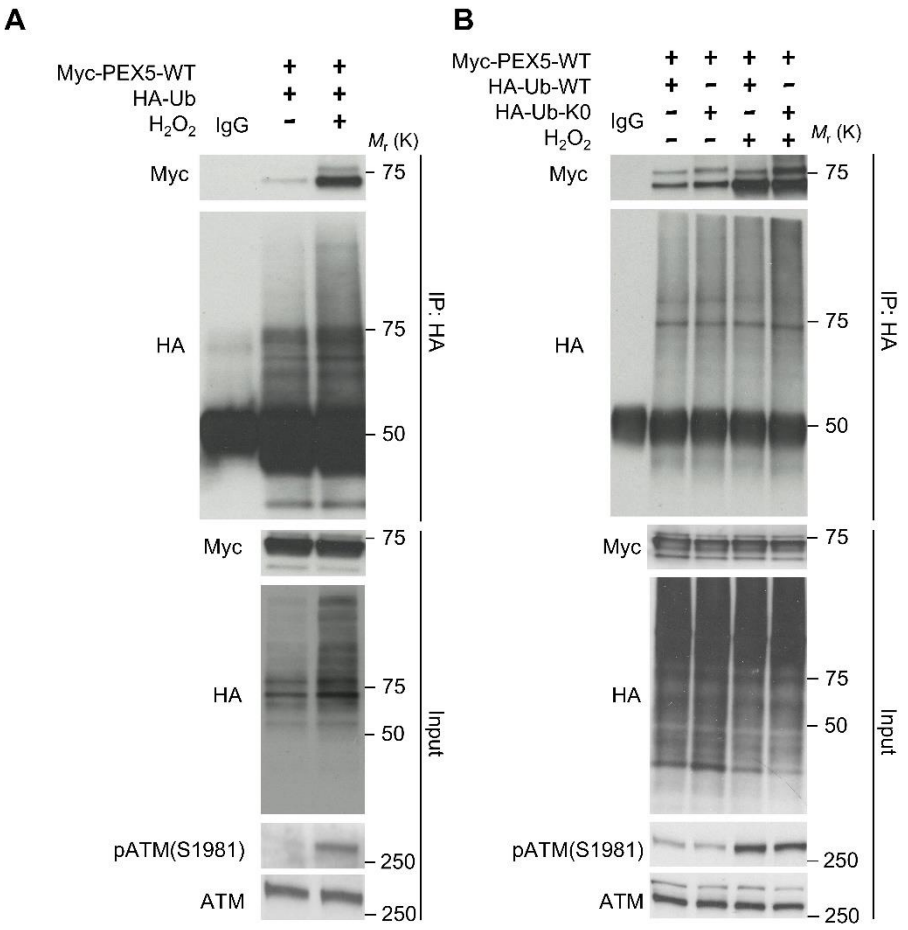

Figure 2. 6 PEX5 is ubiquitinated in response to ROS.

A. HEK293 cells expressing Myc–PEX5-WT and HA–Ub treated with H_2O_2 (0.4 mM) for 6 h were co-immunoprecipitated using anti-HA and blotted using anti-Myc antibody. The inputs were immunoblotted using the indicated antibodies. **B.** HEK293 cells expressing Myc–PEX5-WT and HA–Ub-WT or HA–Ub-K0 (ubiquitin with all lysine residues mutated to arginine) constructs were treated with H_2O_2 (0.4 mM) for 6 h, and Myc–PEX5 co-immunoprecipitated using anti-HA and blotted using anti-Myc antibody. Inputs were immunoblotted using the indicated antibodies.

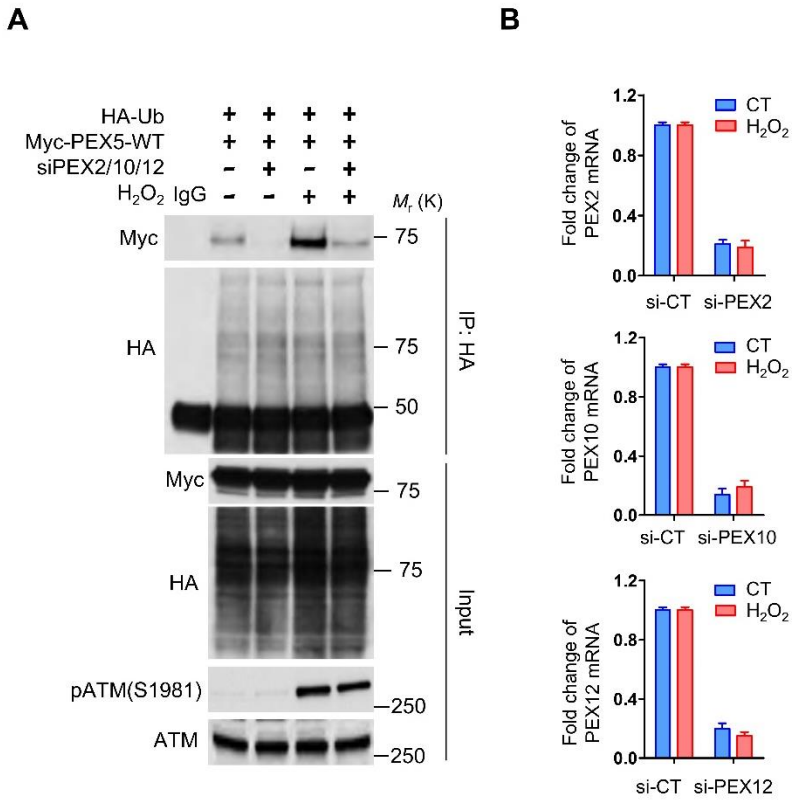

Figure2. 7 PEX2, PEX10 and PEX12 are E3 ligase for PEX5 ubiquitination.

A. HEK293 cells transfected with Myc-PEX5-WT/Myc-PEX5-K209R and HA-Ub constructs for 24 h following a prior siRNA knockdown of PEX2/10/12 for 48 h were immunoprecipitated with anti-HA and immunoblotted with anti-Myc antibodies. Input lysates were immunoblotted using the indicated antibodies. **B.** RT-PCR was performed to confirm siRNA knockdown of PEX2, PEX10 and PEX12.

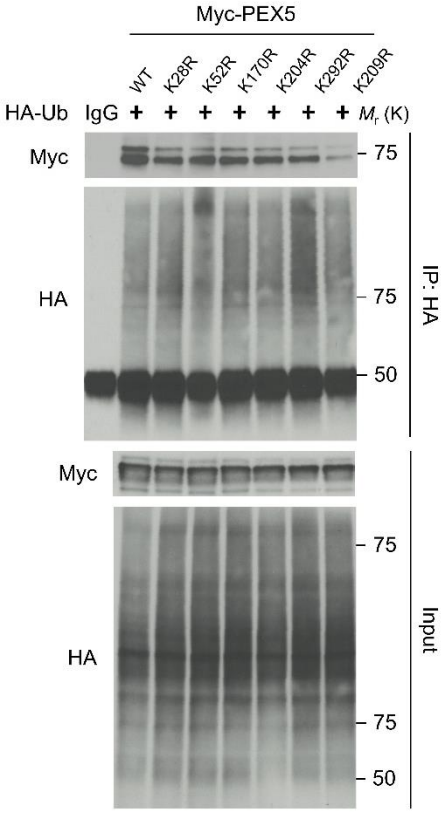

Figure 2. 8 PEX5 is ubiquitinated at Lys209.

HEK293 cells expressing Myc-PEX5-WT or PEX5 mutants (K28R, K52R, K170R, K204R, K209R, K292R) and HA-Ub constructs were co-immunoprecipitated using anti-HA and blotting with an anti-Myc antibody. Input lysates were immunoblotted using the indicated antibodies.

next asked whether phosphorylation of PEX5 by ATM regulated PEX5 ubiquitination in response to ROS. We co-expressed WT and phosphorylation-deficient mutant S141A (mutation of the ATM phosphorylation site) with HA-Ub. We found that Ser 141 mutation in PEX5 abrogated the increase in

ubiquitination of PEX5 in response to ROS (Figure 2. 9A), indicating that ATM phosphorylation PEX5 at Ser141 regulated ROS-induced PEX5 ubiquitination. We observed low background levels of PEX5 ubiquitination with both WT and S141A PEX5 (Figure 2. 9A), suggesting there may be other sites of ubiquitination that are not dependent on ATM phosphorylation at Ser 141, nor ROS-responsive. Furthermore, ROS-induced ubiquitination of endogenous PEX5 was deficient with ATM knock-down with siRNA (Figure 2. 9B). Together, these data indicate that PEX5 ubiquitination is dependent on ATM phosphorylation**.**

ROS-induced p62 and PEX5 interaction

Many autophagy adaptors have been identified, including p62/SQSTM1, NBR1, and NDP52. Only adaptor p62, which contains both LIR (autophagosome) and UBA (ubiquitin) binding domains, has been implicated in selective degradation of peroxisomes in mammalian cells, leading us to ask whether ROS induces p62 and PEX5 interaction. We observed that endogenous PEX5 could be co-immunoprecipitated with endogenous p62, and this interaction was enhanced by ROS (Figure 2. 10A). In agreement with this data, the interaction between exogenous PEX5 and exogenous p62 was increased by ROS (Figure 2. 10B).

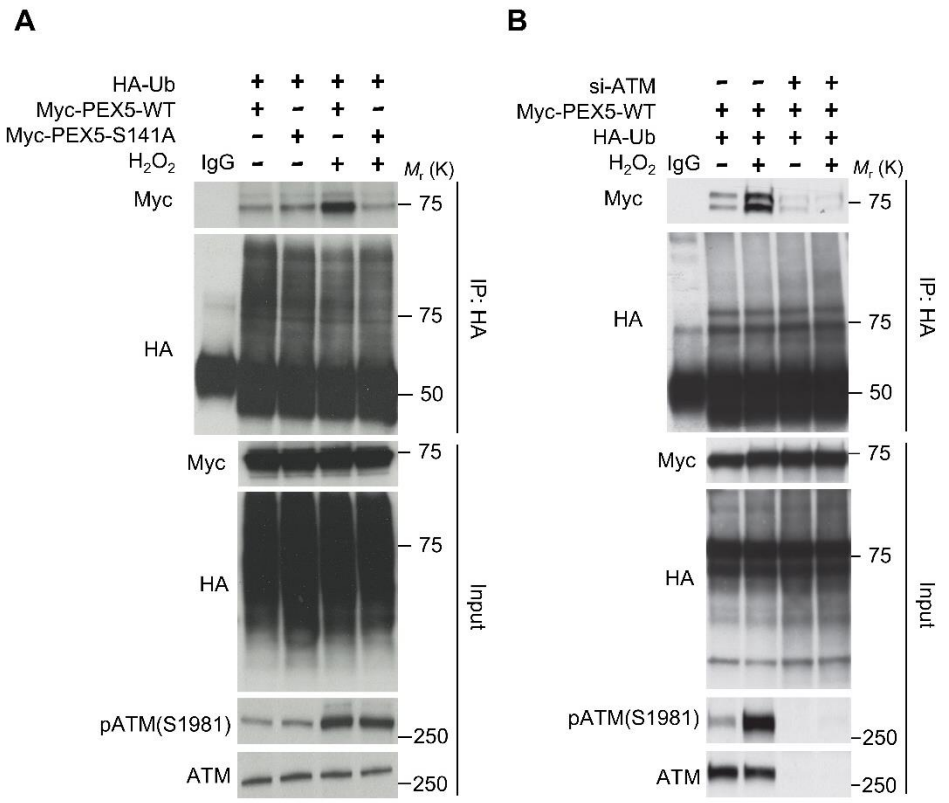

Figure 2. 9 ROS-induced PEX5 ubiquitination is ATM-dependent.

A. HEK293 cells expressing HA-Ub-WT and Myc-PEX5-WT or Myc-PEX5-S141A constructs were treated with H_2O_2 (0.4 mM) for 6 h, and Myc-PEX5 co-immunoprecipitated using anti-HA antibody and blotted using anti-Myc antibody. Input lysates were immunoblotted using the indicated antibodies. **B.** HEK293 cells transfected with Myc-PEX5-WT and HA-Ub for 24 h following a prior siRNA knockdown of ATM for 48 h, were treated with H_2O_2 for 6 h and immunoprecipitated with anti-HA and immunoblotted withanti-Myc antibodies. Input lysates were immunoblotted using the indicated antibodies.

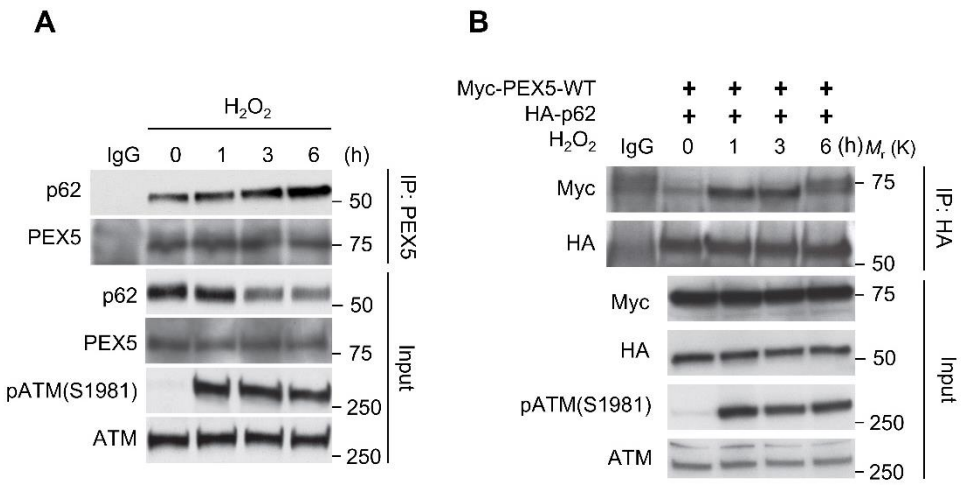

Figure 2. 10 p62 interacts with PEX5.

A. HepG2 cells treated with 0.4 mM of H_2O_2 for the indicated time points were immunoprecipitated with anti-PEX5 and immunoblotted with anti-p62 antibodies. Inputs were immunoblotted using the indicated antibodies. **B.** HEK293 cells were transfected with Myc- PEX5-WT andHA-p62, and treated with 0.4 mM of H_2O_2 for indicated times. The complex of HA-p62 and Myc-PEX5 was immunoprecipitated with anti-HA and immunoblotted with anti-Myc. Inputs were immunoblotted using the indicated antibodies.

Ubiquitinated PEX5 binds to p62 to target peroxisomes for pexophagy

We next tested whether the autophagy adaptor p62 recognizes ubiquitinated PEX5 to mediate peroxisome targeting to the autophagosome. Co-localization of ubiquitinated PEX5 and p62 was increased by ROS in HepG2 liver cells (Figure 2. 11A). ROS-induced p62 tethered to peroxisomes was confirmed by co-localization of p62 with the peroxisomal membrane marker

PMP70 in HepG2 liver cells (Figure 2. 11B). Furthermore, p62 localization to the peroxisome fraction of HEK293 cells was decreased by K209R PEX5 (Figure 2. 11C), concomitant with decreased p62 binding to K209R compared to WT PEX5 (Figure 2. 11D). Together, these data demonstrate that the autophagy adaptor protein p62 binds to PEX5, and that ROS-mediated ubiquitiylation at Lys 209 is necessary for tethering p62 to peroxisomes.

Induction of pexophagy by ROS

Pexophagy is a major process for the prevention of excessive peroxisome number. In order to monitor autophagic flux of pexophagy in response to ROS, we transfected construct in HepG2 cells with differential pH stability, EGFP-mRFP-SKL, and we observed accelerated degradation of peroxisome-localized EGFP- relative to mRFP (Figure 2. 12A)[81]. In response to ROS, there was relatively weak fluorescence of EGFP, indicating that peroxisomes engulfed by autophagosomes fused with lysosomes in cells undergoing pexophagy (Figure 2. 12B). Consistent with induction of pexophagy by ROS, expression of the peroxisomal proteins PEX1 and PEX14 were significantly decreased over time by H_2O_2 treatment (Figure 2. 12C, D) and this decrease was blocked with the lysosomal inhibitor Bafilomycin A1, indicating that the decrease in PEX1 and PEX14 was due to increased autophagic flux (Figure 2. 12E). ROS-induced pexophagy was further confirmed by electron microscopy (Figure 2. 13).

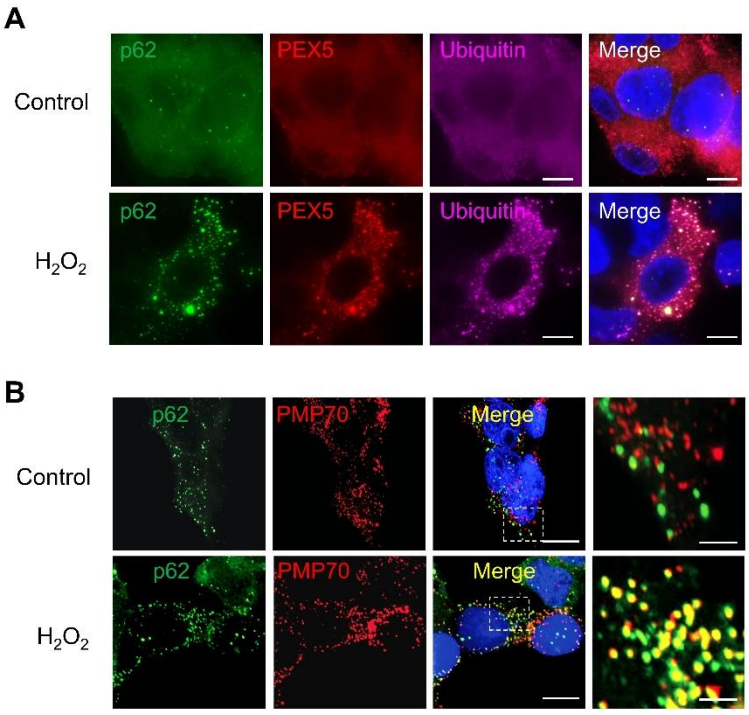

Figure 2. 11 Ubiquitinated PEX5 binds with the autophagy adaptor protein p62 in response to ROS.

A. Representative images of HepG2 cells treated with 0.4 mM of H_2O_2 for 3h and immunostained with p62 (green), PEX5 (red), and ubiquitin (purple). Scale bar, 10µm. **B.** Representative images of FAO cells treated with 0.4 mM of H_2O_2 for 1h and immunostained with p62 (green) and PMP70 (red). Scale bars, 10 µm. High-magnification images of the outlined areas are shown to the right, scale bars, 2.5 µm. **C.** Subcellular fractionation of HEK293 cells overexpressing Myc-PEX5-WT or Myc-PEX5-K209R treated with 0.4mM of H2O2 for 3h. Immunoblotting was performed with the indicated antibodies. **D.** HEK293 cells transfected with HA–p62 and Myc–PEX5-WT or Myc–PEX5-K209R, and treated with 0.4mM of H_2O_2 for 6 h. Lysates were immunoprecipitated with anti-Myc and immunoblotted with anti-HA antibodies. Inputs were immunoblotted using the indicated antibodies.

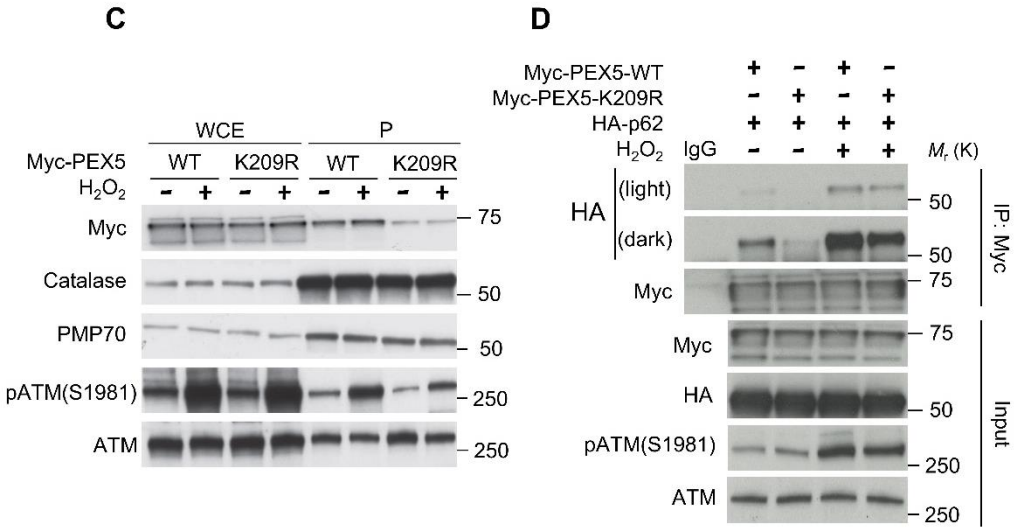

Figure 2. 11. Continued.

Regulation of pexophagy by ROS is ATM and p62 dependent

In previous studies we found that, in response to ROS, ATM induces autophagy by repressing mTORC1 via the TSC2/LKB1/AMPK signaling node[53]. Our data indicate that ATM is localized to the peroxisome by PEX5 and is involved in the regulation of PEX5 phosphorylation and ubiquitination. These data led us to ask whether ATM signaling is involved in the regulation of pexophagy in response to ROS. PEX5-S141A (ATM-phosphorylation deficient), PEX5-S141E (phosphomimetic) or PEX5-K209R (monoubiquitination-deficient) were transfected in PEX5 knockdown cells. The results demonstrated that induction of pexophagy (decreased PEX1 and PEX14) was attenuated in cells expressing the S141A or K209R PEX5 mutants, but not in cells expressing the

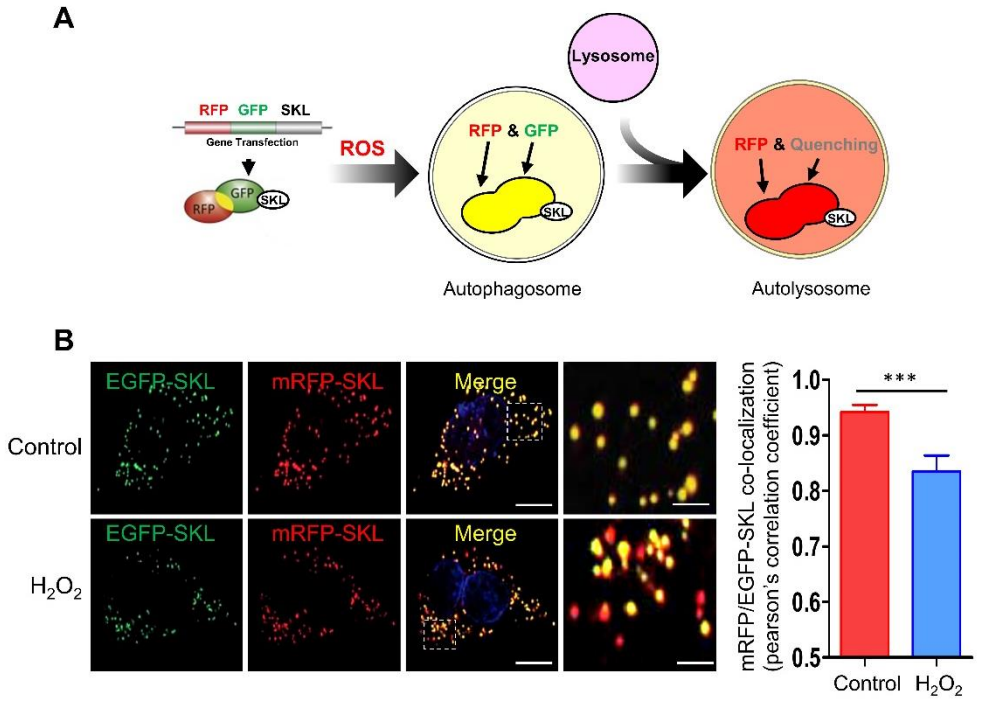

Figure 2. 12 Induction of pexophagy by ROS.

A. The working process interpretation of a tandem SKL fluorescence protein reporter gene system (RFP–GFP–LC3) for peroxisome autophagic flux evaluation. Modified from Yimin Wang,Yu Li,Fujing Wei,Yixiang Duan: Optical Imaging Paves the Way for Autophagy Research. Trends in Biotechnology, 2017, 35(12).* **B.** Representative images using HepG2 cells transfected with an mRFP-EGFP-SKL construct and treated with H_2O_2 (0.4 mM) for 6h. Scale bars 10μm. High-magnification images of the outlined areas are indicated to the right (scale bars, 2.5 μm). The plot on the right shows the Pearson's correlation coefficient for co-localization between mRFP-SKL and EGFP-SKL.

---

* Reprinted with permission from "Optical Imaging Paves the Way for Autophagy Research" by Yimin Wang,Yu Li,Fujing Wei,Yixiang Duan, 2017, Trends in Biotechnology, 35(12), 1181-1193, Copyright [2017] by Elsevier.

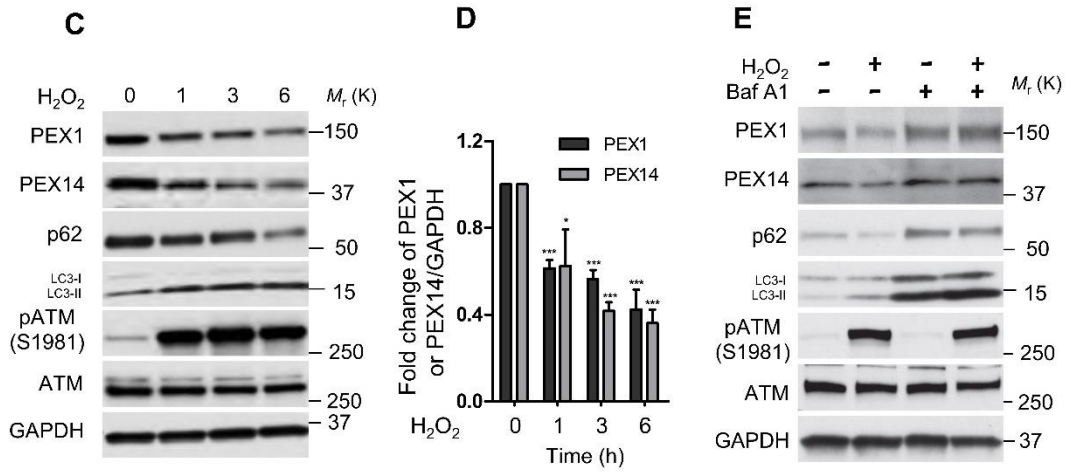

Figure 2. 12 Continued.

C. HepG2 cells treated with either H_2O_2 (0.4 mM) for the indicated times. Western analysis of the peroxisome proteins PEX1 and PEX14 (p62 and LC3-II as autophagy markers). **D.** Quantification of PEX1 and PEX14 intensity normalized to GAPDH. **E.** Western analysis of HepG2 cells pre-incubated in the presence or absence of Bafilomycin A1 (Baf A1, 200nM) for 1h before treatment with H_2O_2 (0.4 mM) for 3h using the indicated antibodies.

S141E phosphomimetic (Figure 2. 14A-C). Interestingly, the S141E mutation alone did not induce PEX1 and PEX14 degradation, indicating phosphorylation (and ubiquitination) is not sufficient to induce peroxisome degradation via selective autophagy. Furthermore, PEX1 and PEX14 protein levels were elevated in ATM-deficient cells in response to ROS (Figure 2. 15A). Consistent with this expectation, we transfected ATM-WT or ATM-KD (kinase dead) in ATM-deficient cells. We observed that pexophagy occurred in ATM-WT cells,

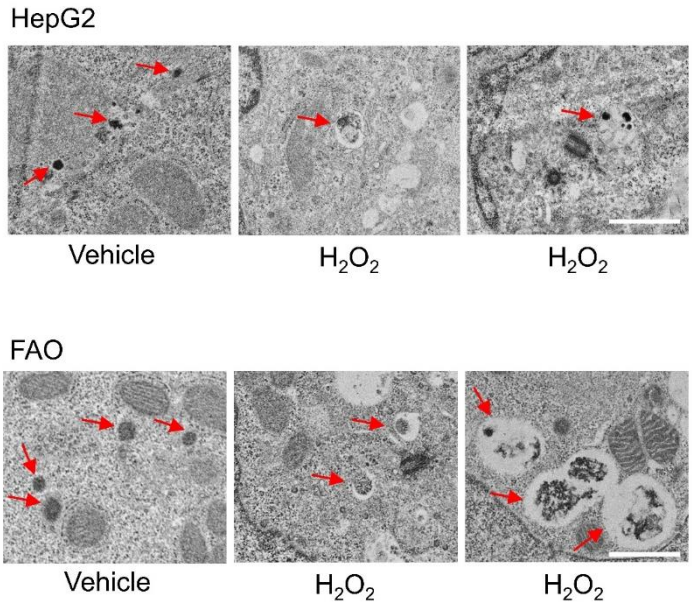

Figure 2. 13 Pexophagy in HepG2 and FAO cells in response to H_2O_2.

Representative electron microscopy images of HepG2 and FAO cells treated with H_2O_2 (0.4mM). Autophagosomes containing peroxisomes are represented by red arrows and shown enlarged in the boxed area (Scale bar, 1 μm).

but not ATM-KD cells (Figure 2. 15B). The decrease in PEX1/PEX14 in response to ROS was abrogated in response to ROS in p62 knockdown cells (Figure 2. 15C-D). All these data indicate that ROS-induced pexophagy is ATM signaling and p62 dependent.

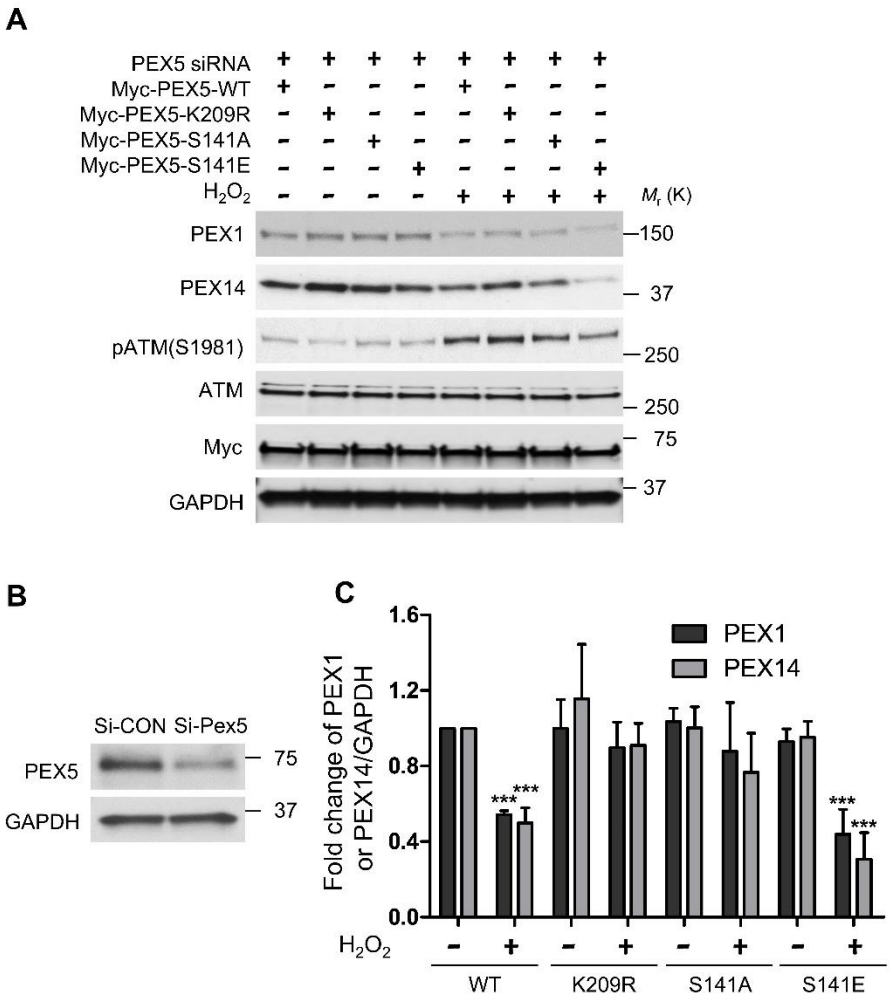

Figure 2. 14 ROS-induced pexophagy is ATM signaling dependent.

A. HEK293 cells transfected with Myc–PEX5-WT or Myc–PEX5-K209R or Myc–PEX5-Ser141 for 24 h following prior siRNA knockdown of PEX5 for 48 h, treated with H_2O_2 (0.4 mM) for 6 h. Western analysis was performed using the indicated antibodies. **B.** Corresponding immunoblots for HEK293 cells transfected with control or PEX5 siRNA showing levels of PEX5. **C.** Quantification of PEX1 and PEX14 intensity normalized to GAPDH from **A.**

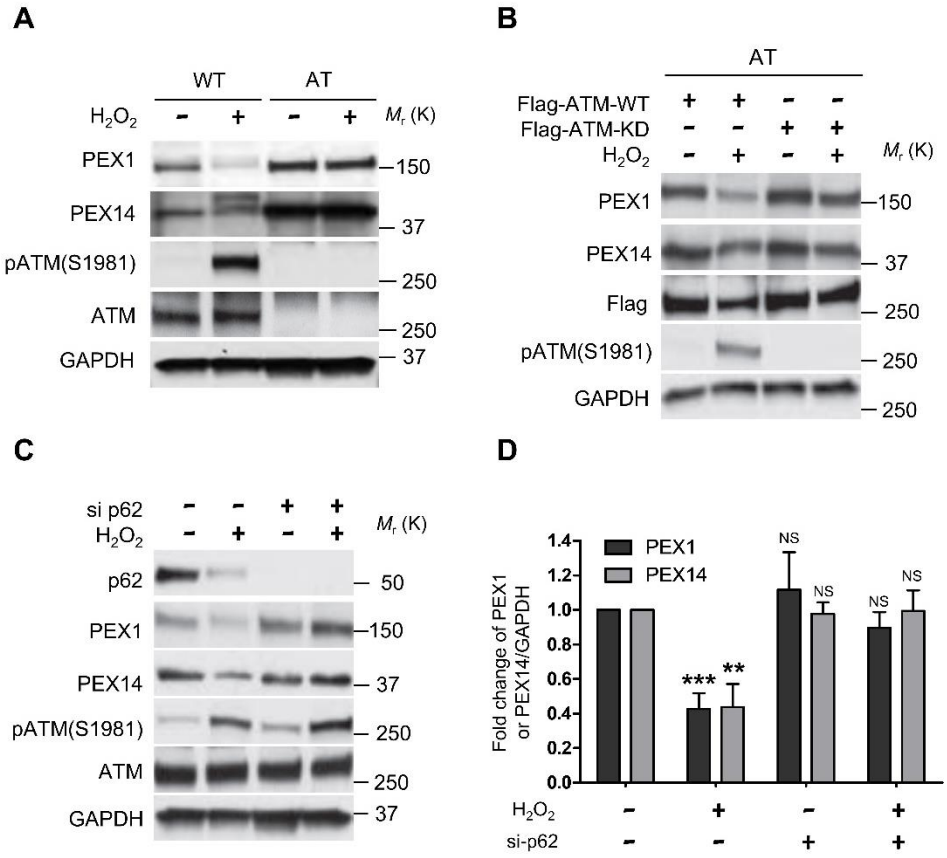

Figure 2. 15 Regulation of pexophagy by ROS is ATM and p62 dependent.

A. WT (GM08399) and AT (GM05849) fibroblasts were treated with H_2O_2 (0.4 mM) for 6 h and immunoblotted with the indicated antibodies. **B.** Western analysis of AT (GM05849) fibroblasts transfected with Flag-ATM WT or Flag-ATM KD (kinase dead) mutant and treated with 0.4 mM H_2O_2 for 6 h using the indicated antibodies. **C.** Western analysis of HepG2 cells transfected with or without si p62 for 72 h and treated with 0.4 mM H_2O_2 for 3 h and blotted the indicated antibodies. **D.** Quantification of PEX1 and PEX14 intensity normalized to GAPDH from **C.**

Conclusion and Discussion

Selective autophagy is a major pathway to remove damaged organelles. In mammals, selective autophagy of mitochondria (mitophagy) is well defined. During mitophagy, the mitochondrial outer membrane protein mitofusin 2 is phosphorylated by mitochondrial kinase PINK1, inducing its ubiquitination by recruiting the E3 ligase parkin[82,83] to trigger mitophagy[84]. Mitophagy reveals a good model for the degradation of other organelles, including the peroxisome illustrating that showing autophagy receptors play a key role in initiating the formation of autophagosome around the organelles. Peroxisomes are autonomously replicating organelles and maintenance of peroxisome homeostasis is crucial for normal cellular functions. Too few peroxisomes cause pathologies collectively known as PEDs and PBDs. Overload of redox enzymes, such as D-amino acid oxidase, may cause oxidative damage and promote diseases such as cancer. In this chapter, we identify a key role for ATM signaling in the regulation of peroxisomal autophagy in response to ROS.

In our previous studies, we identified that the peroxisome is an important functional site for the TSC tumor suppressor. Our recent studies presented here, provided evidence for cross talk between ATM and the TSC tumor suppressor occurring at the peroxisome in response to ROS. ATM is recognized and bound by the PEX5 import receptor, which localizes this kinase to the peroxisome. In response to ROS, ATM is activated, suppressing mTORC1 in a LKB1-AMPK-TSC2 dependent signaling pathway to activate ULK1 and trigger autophagy[85].

Concomitant with activation of ULK1, PEX5 is phosphorylated at Ser141(Figure 2. 5), leading to mono-ubiquitination of peroxisome-localized PEX5 at Lys209 (Figure 2. 8) by the peroxisomal E3 ligase PEX2/10/12 (Figure 2. 7) in an ATM-dependent manner (Figure 2. 9). Subsequently, ubiquitinated PEX5 is recognized by the ubiquitination adapter protein p62, tethering autophagosomes to peroxisomes to induce peroxisomal autophagy (Figure 2. 10-15). Overall, we have identified a model for peroxisomal ATM signaling to induce peroxphagy in response to ROS (Figure 2. 16).

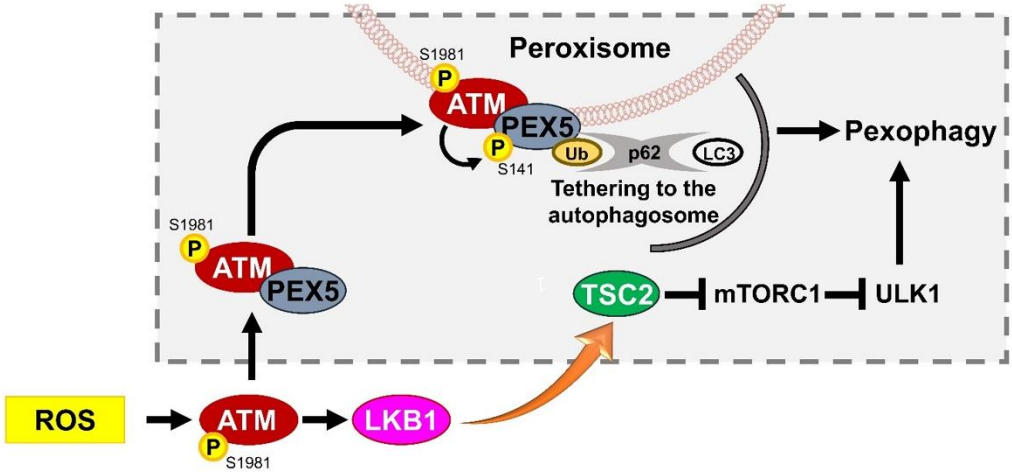

Figure 2. 16 Working model for ATM signaling on peroxisome.

ATM represses mTORC1 through TSC signaling node to, phosphorylation of PEX5 to induce ubiquitination by PEX2/10/12 R3 ligase, and recognition of Ub-PEX5 by p62 to induce pexophagy in response to ROS.

PEX14 has also been reported to directly bind LC3-II under starvation conditions[86]. Moreover, overexpression PMP34 or PEX3 fused with an ubiquitin on the cytosolic face of, is sufficient to trigger peroxisomes turnover[49]. Whether these peroxisomal proteins are also targets of the ATM kinase, or regulated by other, yet to be identified. Furthermore, PEX14 as a docking protein on peroxisomal membrane plays a key role for recruiting the PTS1-PEX5 complex to the peroxisome[87]. It is possible that PEX14 serve as dual roles for PTS1 protein peroxisomal translocation and pexophagy. In addition to p62, NBR1 and NDP52 can also participate in mammalian autophagy[48,49], suggesting that other pathways for selective autophagy of peroxsiomes may also exist.

Peroxisomes also carry a tremendous liability for the cell, as they generate reactive nitrogen species (RNS) as another byproduct. In a previous study, our group identified that RNS regulates ATM-AMPK-TSC2-mediated suppression of mTORC1 and induce autophagy[88]. This suggests the interesting possibility that ATM may also be activated by RNS to repress mTORC1 on peroxisome to deduce peroxisome turnover.

CHAPTER III

AMPK REGULATES PEROXISOMAL CARGO PROTEINS IMPORT VIA PEX5 PHOSPHORYLATION IN RESPONSE TO LOW ENERGY

Introduction

Peroxisomal cargo proteins import.

Peroxisomes are devoid of DNA. All peroxisomal proteins are encoded in the nucleus, and are subsequently synthesized on free ribosomes in the cytoplasm and post-transported into the organelles. Peroxisomes can import completely folded and oligomeric proteins[89]. A major breakthrough in the elucidation of the mechanism of protein import into peroxisomes was the identification of the first peroxisomal targeting signal (PTS1) at the C-terminus consisting of a conserved tripeptide, usually with the consensus sequence (S/A/C)-(K/R/H)-L[15,16]. Very few peroxisome matrix proteins destined for translocation into peroxisomes contain the PTS2 motif, which comprises a nonapeptide with the consensus sequence sequence (R/K)-(L/V/I)-X_5-(H/Q)-(L/A) at the N-terminus. [17,18]. PTS1 is recognized by PEX5, while the receptor for PTS2 is PEX7. In mammals, there are two major isoforms of PEX5: PEX5 short isoform (PEX5S) and PEX5 long isoform (PEX5L), which differs from the short one by inserting of 37 residues at the N-terminus. There is a PEX7 receptor binding site on PEX5L that is required for PTS2 protein peroxisomal destination.

Lack PEX5L fail to import both PTS1 and PTS2-terminated proteins[90]. In contrast to matrix protein import, the mechanisms of PMPs translocation remains poorly defined. There is evidence that PEX3 and PEX19 are involved in PMPs transport in mammals and most yeast species[21,91].

In general, there are four steps per cycle for PEX5-dependent recruitment to PTS1 cargo proteins to the peroxisomal matrix: i) recognition; ii) integration into the peroxisomal membrane; iii) release into the peroxisomal lumen; and iv) receptor recycling back to the cytosol[92]. Upon cargo protein recognition, PTS1-containing proteins are recognized by PEX5 in the cytosol via PEX5 C-terminal seven tetratricopeptide repeats (TPRs) region (Figure 3. 1).

Segments within this region contain two TRP triplets, TPRs 1-3 and TPRs 5-7, that form a “ring” like structure that recognizes PTS1 cargo proteins. TPR4 is a “hinge” region that enables the two TRP triplets to completely surround a single PTS1 containing peptide[93]. A recent study showed that replacement of the asparagine side chain with Lysine in TPR region, such as N489K, would abrogate ligand recognition[93], while a N526K mutant mimics PEX5 binding with PTS1 cargo proteins by triggering a conformation switch in the TRP region. The PTS1 cargo-PEX5 complex is then docked by peroxisomal membrane peroxins PEX13 and/or PEX4 (in mammals) through PEX5 N-terminal pentapeptide WxxxF/Y motif, followed by translocation of the complex into the luminal side of peroxisomal membrane and dissociation of the PTS1 cargo-PEX5 complex[87,94]. Finally, PEX5 undergoes mono-ubiquitination Cys11 by PEX4 and PEX2[74] and

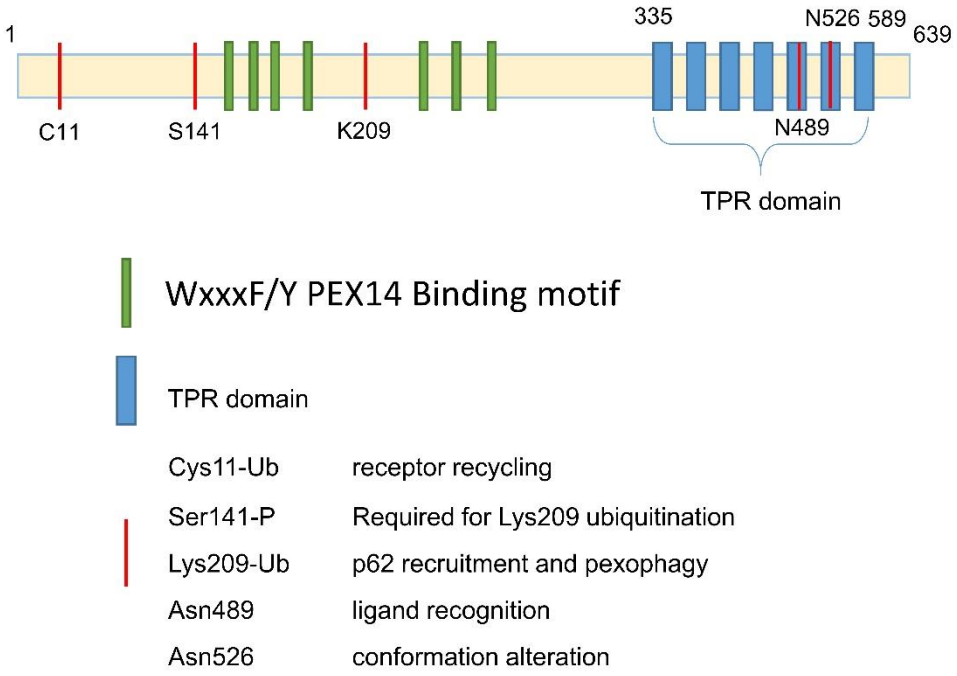

Figure 3. 1 Schematic presentation of the domain structure of the human PEX5 receptor and interaction sites for known components of the PEX5 docking complex.

the subsequently exported from the peroxisomal membrane back to the cytosol for another cycle of import in an AAA ATPase (PEX1 and PEX6) and ATP hydrolysis dependent manner[95].

As a site of metabolism, the peroxisome includes appproximately 50 identified peroxisomal enzymes that contribute to several crucial metabolic processes as such as β-oxidation of fatty acids, biosynthesis of ether phospholipids, and metabolism of ROS. Recent studies have indicated that peroxisome function and dysfunction are associated with a wide variety of age-

related maladies, including cancer, type 2 diabetes, and neurodegeneration.[5,28] Although many peroxisomal enzymes and metabolic pathways are well defined, the mechanisms of regulation of peroxisomal enzymes and their recognition by import receptor(s) have not been elucidated, leaving the regulation of delivery of peroxisomal metabolizing enzymes to the peroxisomal matrix an enigma.

AMPK: A central metabolic regulator.

AMPK is a key regulator of energy balance and is expressed ubiquitously in eukaryotic cells. Genes encoding AMPK subunits are found in essentially all eukaryotes. AMPK is an obligate heterotrimer, containing a catalytic α-subunit, a scaffolding β-subunit and a regulatory γ-subunit.[96,97] The catalytic α-subunit is composed of a conventional serine/threonine kinase domains at the N-terminus, containing a threonine residue (Thr172) that phosphorylation by upstream kinases[98]. Cellular energy stress leads to convert ATP to ADP, some of which is converted to AMP by the adenylate kinase reaction (2ADP↔ATP+AMP), then AMP activates AMPK by binding to the AMPK γ-subunit, which promotes AMPK phosphorylation at Thr172 by LKB1 and inhibits its de-phosphorylation[99]. Although allosteric activation is only caused by AMP, it has recently been found that this effect of AMP was mimicked by binding of ADP[100]. Two upstream kinases, LKB1[101] and CaMKKβ[102] (Ca^{2+}/calmodulin-dependent protein kinase β), phosphorylate Thr-172 of the AMPKα subunit. Once activated, AMPK acts to restore energy homeostasis by promoting catabolic pathways, resulting in ATP

generation, and inhibiting anabolic pathways that consume ATP[103]. Another important aspect of AMPK biology is the role of AMPK in autophagy, a lysosome-dependent catabolic program that maintains cellular homeostasis[104]. A number of studies have demonstrated that AMPK plays an important role in autophagy regulation by directly phosphorylating two autophagy-initiating regulators: the protein kinase complex ULK1[105,106] (Unc-51-like autophagy-activating kinase) and the lipid kinase complex PI3KC3/VPS34[107] (phosphatidylinositol 3-kinase, catalytic subunit type 3; also known as VPS34). Given the functional attributes of AMPK in energy (glucose/lipid) homeostasis, body weight, food intake, insulin signaling and autophagy, AMPK is considered to be a major therapeutic target for the treatment of metabolic diseases including type 2 diabetes and obesity. A number of studies have shed light on the role of AMPK in tumorigenesis[108].

AMPK is a highly selective kinase that strongly prefers basic residues in the -3 and -4 positions and hydrophobic residues at the -5 and +4 positions or both[109,110]. This suggests that proteins that have this signature sequence are likely to be authentic substrates of AMPK. This was confirmed by the first peptide substrate for AMPK acetyl-CoA carboxylase-1 (ACC1) at Ser79[110] and mTOR binding partner raptor on Ser792[109]. Thus we can use the optimal AMPK substrate motifs to mine protein databases for matching sequences to identify candidate substrates.

Our previous studies showed that ATM suppresses mTORC1 in a TSC2-dependent signaling pathway via LKB1 and AMPK to activate ULK1 and trigger selective autophagy of peroxisomes in response to ROS/RNS. My work, in chapter III continues this line of study, focusing on uncovering novel kinases (with focus on AMPK) at the peroxisome, and investigating if 1) the peroxisome is a signaling organelle involved in the AMPK signaling pathway, and 2) AMPK phosphorylation of PEX proteins (with focus on PEX5) affects delivery of peroxisomal matrix proteins to the peroxisome to regulate its homeostasis or functions.

Materials and Methods

Antibodies

The following antibodies were used: phospho-AMPK (Thr 172; no. 2531, 1:500 WB), AMPK (no. 2532, 1:500 WB), lamin A/C (no. 2032, 1:1,000 WB), HA (no. 3724, 1:2,000 WB), TSC2 (no. 4308, 1:2,000 WB), phospho-(S/T) AMPK substrates (no. 5759, 1:1,000 WB), phospho-ACC (no. 3661L, 1:1,000 WB), ACC (no. 3662S, 1:1,000 WB) were purchased from Cell Signaling Technology. Phospho-ATM Ser 1981 (ab81292, 1:1,000 WB), catalase (ab1877, 1:5,000 WB, 1:500 IF), and HA (ab9110, 0.5 g per 100 g of total protein for immunoprecipitation (IP)) were purchased from Abcam. c-Myc (9E10; sc-40, 1:2,000 WB, 2 g per 100 g of total protein for IP), GAPDH (SC-25778, 1:5,000 WB), ATM (SC-23921 1:1,000 WB), PEX5 (SC-23188 1:300 IF) were purchased from Santa Cruz Biotechnology. Other antibodies used in this study are as follows: phospho-PEX5 (Ser 141) and PEX5 (Ser 279) were synthesiszed by Covance. PEX5 (no. 12545-1-AP, 1:1,000 WB, 1:200 IF) were purchased from Proteintech. Flag (F3165, 1:4,000 WB, 1:500 IF, 1.25 g per 100 g of total protein for IP) and PMP70 (SAB4200181, 1:5,000WB, 1:500 IF) were purchased from Sigma. ATM (GTX70103, 1:1,000) was from GeneTex; LDH (AB1222, 1:2,000 WB) was from Chemicon; β-integrin (no. 610468, 1:2,000 WB) was from BD Transduction Laboratories; Secondary antibodies (1:2,000) conjugated to horseradish peroxidase were purchased from Santa Cruz Biotechnology.

Secondary antibodies for immunofluorescence staining, anti-mouse, -goat and -rabbit Alexa Fluor 488, 546 and 633 were obtained from Molecular Probes (1:1,000). Reagents are as follows: hydrogen peroxide solution (323381-25ML) and 2-Deoxy-D-Glucose (2-DG) were purchased from Sigma.

Cell culture and transfection

HEK293T (ATCC) cells were maintained in DMEM supplemented with 10% FBS. HepG2 (ATCC) cells were cultured in MEM supplemented with 10% FBS. Transient transfections were performed using the Lipofectamine 2000 reagent (Invitrogen) according to the manufacturer's instructions. All of the cell lines were also tested and confirmed negative for mycoplasma.

Plasmids and mutagenesis

Full length human PEX5 was subcloned into pJET1.2/blunt cloning vector with SalI restriction sites to amplify full-length hPEX5. Myc-tagged hPEX5 was made by inserting amplified fragments, using SalI restriction sites, into the pCMV-Myc expression vector. Flag-PEX5 was generated through Gateway cloning (Life Technologies). A series of mutant constructs of PEX5 were generated by the QuikChange Lightning Multi Site-Directed Mutagenesis Kit. The primers for different sites were designed as follows (Table 3.).

Immunoprecipitation and western blotting assay

The cells were washed in cold PBS 3 times and lysed in cold CST lysis

Table 3. Primers for mutagenesis

Gene Name		Sequence (from 5'-3')
hPex5-S279A	Forward	GTTTGAACGAGCCAAGGCAGCTATAGAGTTGCAG
	Reverse	CTGCAACTCTATAGCTGCCTTGGCTCGTTCAAAC
hPex5-S621A	Forward	GACGCGCGGGATCTGGCCACCCTCCTAACTATG
	Reverse	CATAGTTAGGAGGGTGGCCAGATCCCGCGCGTC

buffer (20mM Tris-HCl (pH 7.5), 150mM NaCl, 1mM EDTA, 1mM EGTA, 1% Triton X-100, 2.5mM Na pyrophosphate, 1mM β-glycerophosphate) containing 1 × protease inhibitor cocktail and phosphatase inhibitor cocktail 2 and 3 (Sigma). Rotate the cell lysates at 4 ℃ for 30 min, and centrifuge at 4 ℃ at maximum speed (10,000g) for 10 min. The supernatant was transferred to a new centrifuge tube and subjected to BCA Protein Assay (Thermo Scientific) to quantify protein levels. The cell lysates were used for western blotting with the indicated antibodies. For immunoprecipitation, the cell lysates were immunoprecipitated with the indicated antibodies and incubated with Magnetic A/G beads (Thermo Scientific) overnight at 4 ℃. The beads were pelleted and washed with CST lysis buffer 5 times and were heated in 1× denaturing loading buffer for 10 min at 95 ℃. The immune-complexes were separated on a 4-15% gel (Bio-Rad), transferred to PVDF membranes and probed with indicated antibodies.

AMPK in vitro kinase assay

Grow cells to 70-80% confluency. Myc-PEX5 WT or mutants were transfected into HEK293T cells for 24 hours at 37 ℃, 5% CO_2. Myc-PEX5 WT or mutants were immunoprecipitated with Myc antibody as indicated. Rotate IP samples at 4 ℃ for overnight. The immune-complex was washed with CST lysis buffer (20mM Tris-HCl (pH 7.5), 150mM NaCl, 1mM EDTA, 1mM EGTA, 1% Triton X-100, 2.5mM Na pyrophosphate, 1mM β-glycerophosphate) containing 1 × protease inhibitor cocktail and phosphatase inhibitor cocktail 2 and 3 (Sigma) for 3 times. Then washed with AMPK kinase buffer (25mM MOPS, pH 7.5, 1mM EGTA, 0.1 mM Na_3VO_4, 15mM $MgCl_2$) for 3 times. Immunoprecipitated PEX5 beads were performed in AMPK kinase buffer containing 0.5μg recombinant AMPK (Millipore, #14-840), 100μM cold ATP and 5μCi [γ^{32}] ATP per reaction for 30 min at 30 ℃. Terminate reaction by adding 20 μl 2× protein sample buffer. Boil for 5 min at 95℃. Run samples on a 4-15% gradient gel until the dye front has reached close to bottom. Dry gel for 1 hour at 80 ℃ using a vacuum slab gel dryer. Cover dry gel with plastic wrap and develop gel in indicated time.

Cellular Fractionation assay

Wash and collect cells from 15-cm plates (70-80% confluent) by scraping into ice-cold PBS, and pellet by centrifugation at 1500 rpm for 5min at 4℃. Aspirate the supernatant and resuspend the pellet in 5 volumes of hypotonic buffer containing complete protease inhibitor (10 mM HEPES, pH 7.2, 10 mM

KCl, 1.5 mM $MgCl_2$, 0.1 mM EGTA, 20 mM NaF, and 100 µM Na_3VO_4), and stroke using a Dounce homogenizer for 50-100 times depending on cell type. Crude nuclei and unbroken cells were then pelleted (termed pellet A) by centrifugation at 3,000 rpm at 4℃ for 5 min. The supernatant A was separated by ultracentrifugation at 29,000 rpm for 1 h at 4℃. Collect the supernatant B, or cytosolic fraction. The pellet B (membrane containing fraction) was lysed in 1× CST lysis buffer (as above) containing complete protease inhibitor. Remove the insoluble fractions by centrifugation at max speed for 10 min at 4 ℃, then get supernatant C (membrane lysate). Crude nuclei (pellet A) were resuspended with hypotonic buffer containing complete protease inhibitor and homogenized using a Dounce homogenizer. Discard the supernatant by centrifugation at 3000 rpm for 5 min at 4℃. Wash the pellet with nuclear wash buffer (10 mM Tris-HCl, pH 7.4, 0.1% NP-40, 0.05% Na-Deoxycholate, 10 mM NaCl, and 3 mM $MgCl_2$). The pellet (nuclear fraction) was lysed in high salt lysis buffer (20 mM HEPES, pH 7.4, 0.5 M NaCl, 0.5% NP-40, and 1.5 mM $MgCl_2$).

Peroxisome Isolation

Peroxisome isolation was performed using the Peroxisome Isolation Kit (Sigma) according to the manufacturer's protocol. Briefly, cells were washed by scraping into ice-cold PBS to remove the serum. Pellet cells at 1,200 rpm for 5min at 4℃ and discard the supernatant. The cells were resuspended in 1× Peroxisome Extraction Buffer, broke the cells in Dounce homogenizer, and

centrifuged at 1,000 g for 10 minutes. Transfer the supernatant to a new centrifuge tube and centrifuge at 2,000 g for 10 minutes. Collect the supernatant and further centrifuge at 25,000 g for 20 minutes. Resuspend the pellet in a minimal volume of 1×Peroxisome Extraction Buffer, and subjected to density gradient centrifugation at 100,000 g for 1.5 hours. The purified peroxisomes were enriched in the bottom layer.

Statistical analysis

The quantitative data are shown as mean ± s.d. Statistical significance was determined with paired Student's t-test between two groups and $P < 0.05$ was considered statistically significant. All experiments were repeated at least three times and representative data are shown as indicated.

These results may reflect the diverse functions of …

The links, if any, between these alternative functions of … remain to be discovered.

Results

PEX5 contains an AMPK substrate motif

To identify AMPK substrates that mediate AMPK effects on peroxisomal function and metabolism, we used a two-part screen to identify AMPK substrates. The known optimal AMPK substrate motif was used to analyze all PEX protein(s) in Peroxisome DB 2.0 for proteins containing conserved candidate target sites. The minimal essential requirement for the AMPK substrates was strong selectivity at the -5, -4, -3, +3, and +4 positions (Figure 3. 2A). Strong selection criteria included: 1) basic residues in the -3 and -4 positions relative to the phospho-acceptor site; 2) hydrophobic residues, including leucine and methionine, in the -5 position and the +4 position, which are consistent with previous studies of the optimal peptide substrates for AMPK based on mutagenesis and molecular modeling; and 3) polar residues in the +3 position, with asparagine, aspartate and glutamate being the most highly selected[109]. Kinase prediction identified potential AMPK phosphorylation motifs in PEX5 at Ser279 and Ser621, but only Ser279 is evolutionarily conserved (Figure 3. 2B). This highly conserved sequence in PEX5, similar to that of other AMPK substrates such as acetyl-CoA carboxylase1 (ACC1) and Raptor, matches the consensus AMPK phosphorylation motif (Figure 3. 2B).

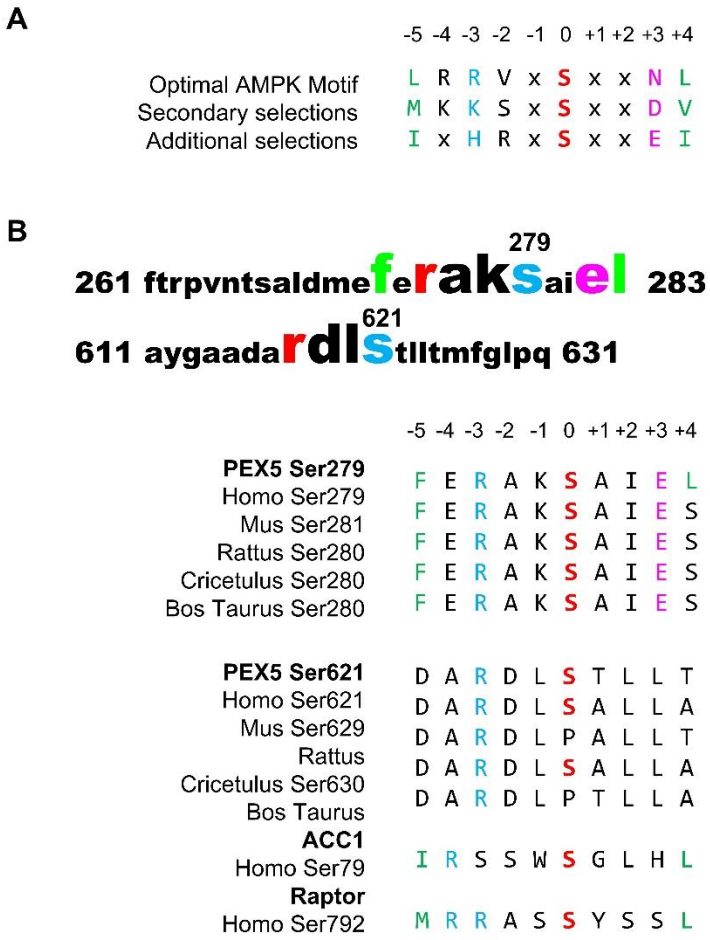

Figure 3. 2 PEX5 with AMPK substrate motif.

A. The structure of optimal AMPK motif. AMPK displayed strong selectivity at the −5, −3, +3, and +4 positions. **B.** PEX5 amino acid sequence. Clustal alignment of Ser 279 and Ser621 in PEX5 matches the optimal AMPK substrate motif.

AMPK phosphorylates PEX5 at Ser279 in response to low energy

Based on *in silico* analyses, we predicted that Ser 279 and Ser 621 of PEX5 are phosphorylated by AMPK. To test this prediction, we used site-directed mutagenesis to generate S279A and/or S621A of PEX5 mutants that cannot be phosphorylated to determine if loss of the S279 or S621 residues abrogates AMPK phosphorylation of PEX5. Using an AMPK-substrate-specific antibody that recognizes S/T sites phosphorylated by AMPK, we found that PEX5 was recognized by this pan-phospho-(S/T) AMPK substrate antibody (Figure 3. 3A). Further, we established *in vitro* kinase assays to test the residue(s) of PEX5 that are phosphorylated by AMPK. Myc-tagged wild-type (WT) PEX5 and mutant (S279A, S621A or S279/621A) PEX5 were immunoprecipitated from HEK293 cells and used as substrates for purified active AMPK in the presence of [^{32}P]-ATP. PEX5 was phosphorylated by AMPK *in vitro* (Figure 3. 3B). Furthermore, mutation analyses identified Ser279 (not Ser621) as the major AMPK phosphorylation site. A search of mass spectrometry databases (http://www.phosphosite.org) revealed that Ser279 of PEX5 has been identified by mass spectrometry as being phosphorylated, confirming Ser279 as a *bona fide* site for PEX5 phosphorylation. We next generated a polyclonal antibody to a phosphor-Ser279 peptide, and used this antibody to confirm that phosphorylation of PEX5 at Ser279 increased in response to low energy (Figure 3. 3C-D) Together, these data demonstrate that PEX5 is directly phosphorylated by AMPK at Ser279.

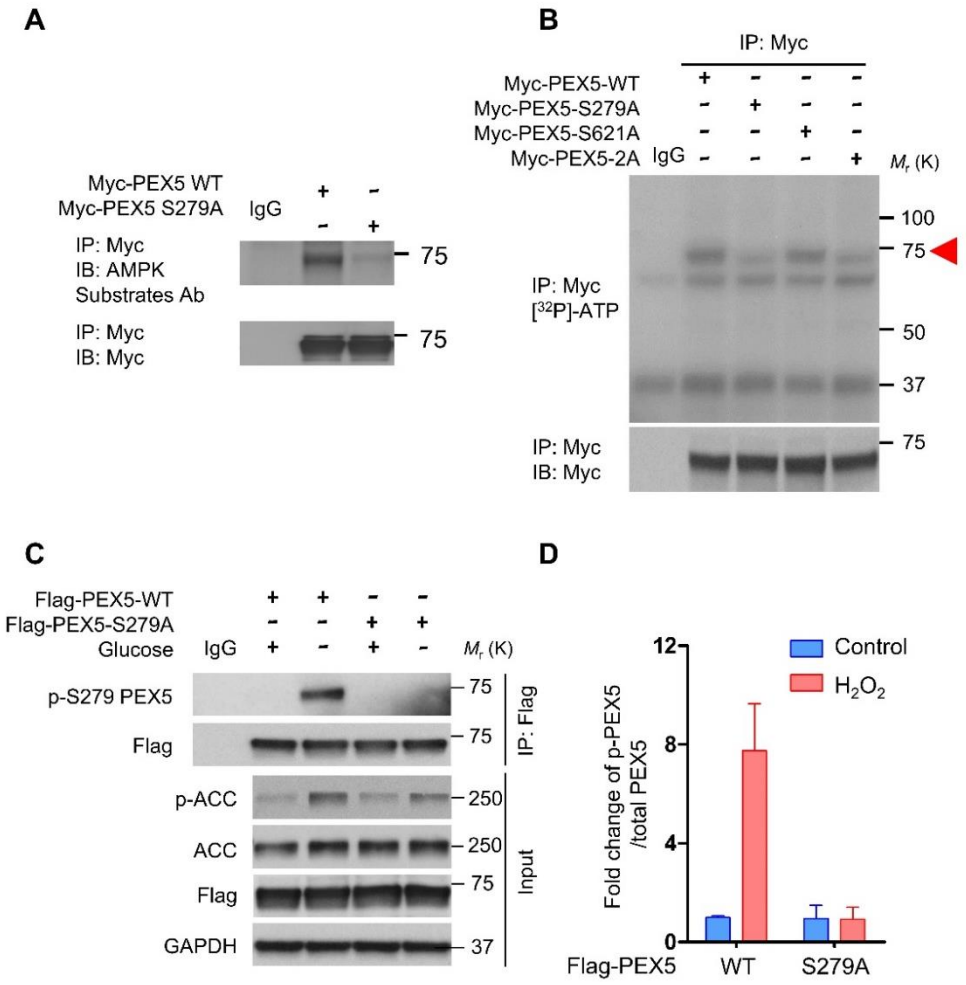

Figure 3. 3 AMPK phosphorylates PEX5 at Ser 279 A.

A. Immunoprecipitation of Myc-PEX5 (WT or mutant) using an anti-Myc antibody followed by immunoblotting with a phospho-AMPK substrate antibody. **B.** *In vitro* kinase assays, Myc-tagged WT PEX5 or mutant (S279A, S621A, or S279/621A) PEX5 that were immunoprecipitated with Myc antibody from HEK293T cells and used as substrates for purified active AMPK in the presence of [^{32}P]-ATP. **C.** HEK293T cells transfected with either a Flag–PEX5-WT or Flag–PEX5-S279A mutant construct. The cells were starved of glucose for 8 hours before lysis. Western analysis was performed with the indicated antibodies. **D.** Quantification of p-S279 PEX5 intensity from **C.**

PEX5 is phosphorylated at Ser 279 in response to ROS

We previously found that PEX5 binds ATM and localizes this kinase to the peroxisome (Chapter II). In response to ROS, ATM signaling activates ULK1 and inhibits mTORC1 via the LKB1-AMPK-TSC2 signaling node to induce autophagy[53]. The specificity for pexophagy is provided by ATM phosphorylation of PEX5 at Ser141, which promotes PEX5 mono-ubiquitination at K209 by the peroxisome E3 ligase PEX2/10/12. Ubiquitinated-PEX5 is recognized by the autophagy adapter protein p62, directing the autophagosome to peroxisomes to induce pexophagy. Since ATM is upstream of AMPK (Figure 3. 4A), PEX5 should be phosphorylated at Ser279 in response to ROS. Indeed, site-directed mutagenesis of Ser279 of Flag-PEX5 to alanine revealed that immunoreactivity with the phosphor-Ser279-PEX5 polyclonal antibody increased with H_2O_2 treatment in Flag-PEX5-WT, but the Flag-PEX5- S279A mutant was not recognized by this antibody (Figure 3. 4B). This suggests that PEX5 is phosphorylated at Ser279 in response to ROS.

PEX5 phosphorylation at Ser279 is independent of Ser141 phosphorylation in response to low energy.

ROS induces PEX5 phosphorylation at Ser279, leading us to predict that phosphorylation of PEX5 at Ser141 is required for phosphorylation of PEX5 at Ser279 by AMPK. Therefore, we next asked whether PEX5 phosphorylation at Ser141 is required for Ser279 phosphorylation in response to low energy.

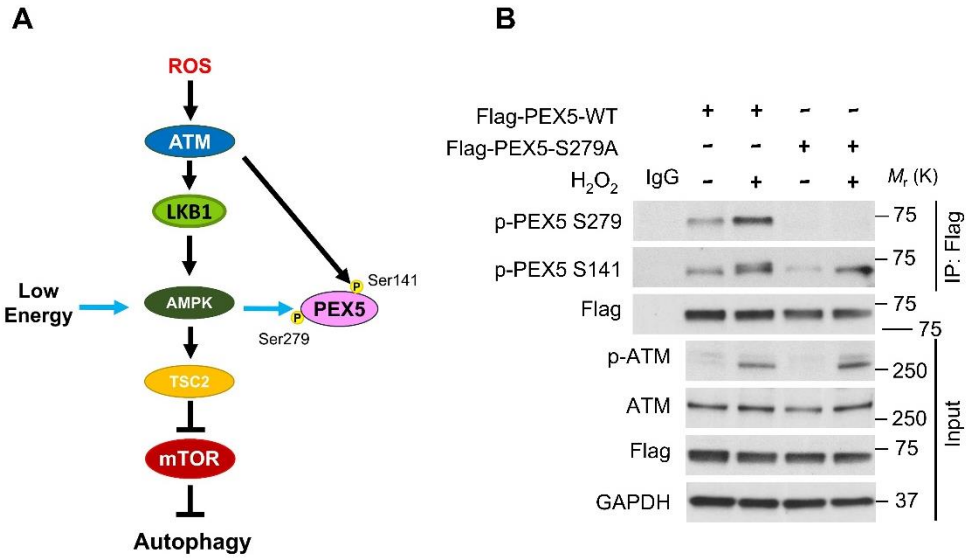

Figure 3. 4 PEX5 phosphorylation at Ser279 in response to ROS.

A. Schematic showing ATM and AMPK signaling pathway in response to ROS or low energy. **B.** HEK293T cells transfected with either a Myc–PEX5-WT or Myc–PEX5-S141A mutant construct treated with H_2O_2 (0.4 mM) for 1 h. Western analysis was performed with anti-pPEX5 (Ser141), Myc, pATM (Ser 1981), ATM and GAPDH antibodies.

We examined PEX5 phosphorylation in response to low energy using Flag-PEX5-WT and Flag-PEX5-S141A. Mutation of the ATM phosphorylation site in PEX5 (S141A) didn't abrogate the increase in phosphorylation of PEX5 in response to low energy (Figure 3. 5A). This result was confirmed by an *in vitro* kinase assay where Myc-tagged wild-type (WT) PEX5 and mutant (S279A or S141A) PEX5 were immunoprecipitated from HEK293 cells and used as

substrates for purified active AMPK in the presence of [^{32}P]-ATP. Ser141 mutant is no affect for PEX5 phosphorylation by AMPK *in vitro* (Figure 3. 5B). This result suggests that PEX5 phosphorylation by AMPK is independent of ATM phosphorylation at Ser141.

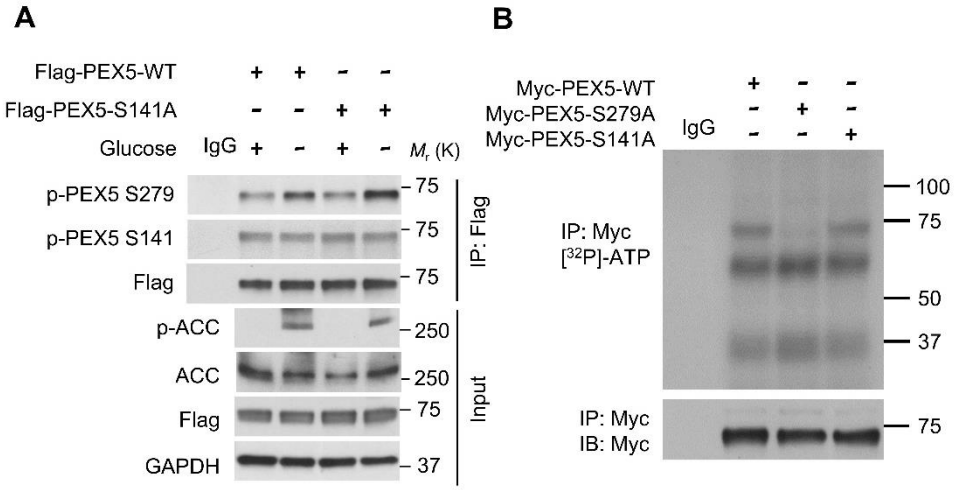

Figure 3. 5 PEX5 phosphorylation at Ser141 is not required for Ser279 in response to low energy.

A. Either a Flag–PEX5-WT or Flag–PEX5-S279A mutant construct was transfected into HEK293T cells. The cells were starved of glucose for 8 hours before lysis. Western analysis was performed with anti-pPEX5 (Ser 279), Myc, pACC (Ser 79), ACC and GAPDH antibodies. **B.** *In vitro* kinase assays, Myc-tagged WT PEX5 or mutant (S279A, or S141A,) PEX5 that were immunoprecipitated with Myc antibody from HEK293T cells and used as substrates for purified active AMPK in the presence of [^{32}P]-ATP.

The PEX5 and ATM/TSC2 interaction in response to low energy

PEX5 recognizes newly synthesized proteins with a PTS1 motif in the cytosol and promotes their translocation across the peroxisomal membrane. However, how PEX5 recognition and translocation of cargo proteins is regulated remains unclear. We have shown that TSC and ATM signaling nodes localize to peroxisomes, where they regulate mTORC1 and peroxisomal degradation in response to ROS[64] (Chapter II). We also identified that TSC2 and ATM were both localized to the peroxisome by PEX5. *In silico* analysis of the TSC2 and ATM (http://peroxisomedb.org) identified a region of homology with a known PTS1 sequence. This ARL motif, ^{1739}KWIARLRHIKR^{1749}, was located 63 amino acids from the C-terminus of the TSC2 protein[64]; ^{3043}KNLSRLFPGWK^{3053} was located 8 residues from the C-terminus of ATM protein (Chapter II) (Figure 3. 6A). Therefore, we hypothesized that PEX5 phosphorylation at Ser279 by AMPK affects TSC2 or ATM cytosolic recognition in response to low energy. To verify this hypothesis, we next investigated PEX5 and TSC2 or ATM interaction in response to low energy. In HEK293T cells transfected with Flag-PEX5-WT or Ser279 mutant, there is no difference in the interaction between PEX5 and TSC2 or ATM in response to low energy (Figure 3. 6B), suggesting that glucose starvation-induced PEX5 phosphorylation at Ser279 is not required for the interaction between receptor PEX5 and the cargo proteins TSC2 and ATM.

A

Protein	Sequence
TSC2	KWI ARL RHIKR
ATM	KNL SRL FPGWKAWV

B

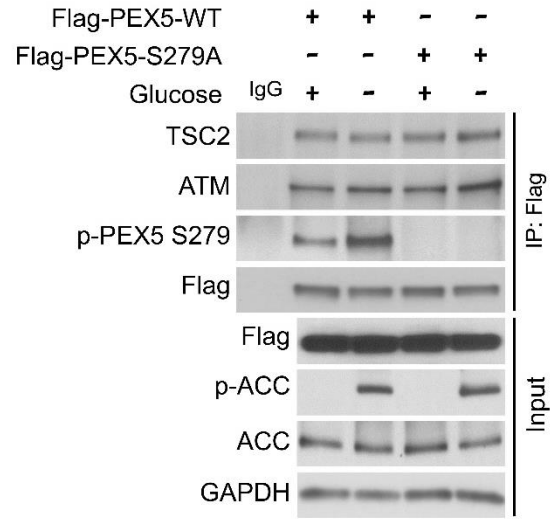

Figure 3. 6 PEX5 interacts with TSC2 or ATM in response to low energy.

A. Peroxisomal proteins with putative PEX5-binding sequence. **B.** HEK293T cells were transfected with either a Flag–PEX5-WT or Flag–PEX5-S279A mutant construct. The cells were starved of glucose for 8 hours before lysis. PEX5 WT or mutant was immunoprecipitated from HEK293T cells with Flag antibody. Western analysis was performed with indicated antibodies.

The TSC2 and ATM peroxisomal distribution in response to low energy

PTS1 containing peroxisomal cargo proteins are recognized by the import receptor PEX5 in the cytosol, which guides them to integrate into the peroxisomal membrane. We observed that Ser279 phosphorylation in response

to low energy did not affect the PEX5 and TSC2 or ATM interaction, however, it is possible that AMPK plays a role in regulating TSC2 or ATM peroxisomal membrane translocation in response to low energy. To explore this possibility, we next examined ATM and TSC2 peroxisomal distribution in response to low energy. Cell fractionation studies showed that TSC2 and ATM localization to the peroxisome fraction of cells was greatly decreased in response to glucose starvation (Figure 3. 7). Taken together, data generated from Chapter III demonstrate that AMPK phosphorylation of PEX5 at Ser 279 regulates delivery of peroxisomal cargo proteins (particularly TSC2 and ATM) to peroxisomes.

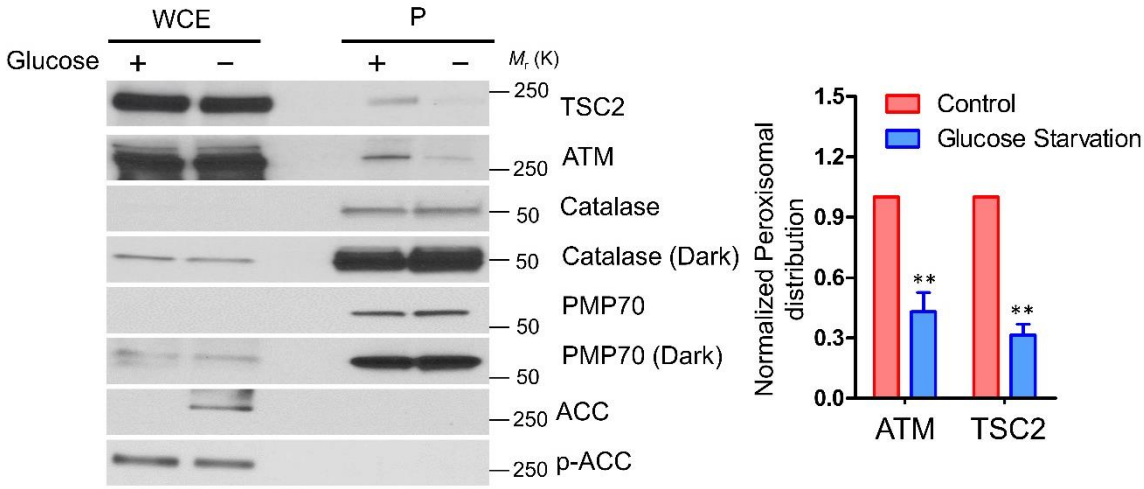

Figure 3. 7 TSC2 and ATM peroxisomal distribution in response low energy

Peroxisome fractionation of HEK293T cells. Catalase and PMP70 were used as subcellular markers of the peroxisome (P). WCE, whole-cell extract. Left panel is quantification of ATM and TSC2 intensity normalized to PMP70 (Student's t-test, $P < 0.01$).

Conclusion and Discussion

AMPK is known to be a major regulator of cellular energy homeostasis, but it has not been linked to the peroxisome, which is the major site for metabolism in mammalian cells. In this chapter, we provide evidence that 1) the peroxisome is a site involved in AMPK signaling; and 2) AMPK phosphorylation of the peroxisomal import receptor PEX5 at Ser279 affects delivery of peoxisomal cargo proteins to the peroxisome (Figure 3. 8). This suggests a model where the AMPK regulates peroxisomal functions and dynamics to yield a better understanding of the crosstalk between AMPK and peroxisomes.

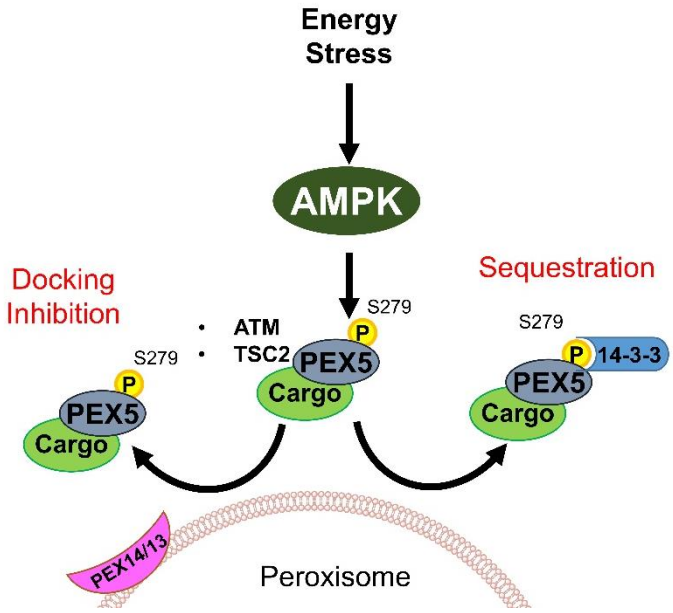

Figure 3. 8 Model for the AMPK regulation of PEX5 phosphorylation and peroxisomal cargo proteins import.

The targeting and import of peroxisomal membrane and matrix proteins requires specific signal sequences, receptors, and translocation machineries. Peroxisomes can import completely folded and oligomeric proteins[89]. The transport of new protein synthesized in cytoplasm to peroxisomes depends on the peroxisomal targeting signal. Two types matrix protein import receptors have been identified: PEX5 and PEX7, which bind with PTS1 and PTS2 motif, respectively. Most matrix proteins contain C-terminal conserved tripeptide PTS1, which is recognized by PEX5[18,19] and they form cargo-receptor complexes in cytosol. Subsequently the complexes are recruited to the peroxisome membrane by the docking sub-complex, PEX13/PEX14, thus, promoting PTS1 proteins import[111]. However, how to regulate PTS1 proteins and PEX5 recognition and how to regulate the cargo-receptor complexes peroxisomal translocation are still not well defined.

I demonstrated here that glucose starvation decreased PEX5 mediated localization of ATM and TSC2 the peroxisome, but had no effort on the interaction of with PEX5 and ATM or TSC2. We have considered two possibilities to potentially explain this phenomenon (Figure 3. 8). One possibility is that 14-3-3 traps the cargo-PEX5 complex in the cytosol, abrogating import by PEX5 and 14-3-3 association. 14-3-3 proteins are conserved regulatory molecules, which could be involved in many different signaling pathways to modulate cellular energy and nutrient dynamic in all eukaryotic cells. Recent studies have been shown that 14-3-3 proteins have the ability to bind numerous

proteins upon phosphorylation by AMPK[112,113]. Using the Scansite program prediction, I found that phosphorylated PEX5 at Ser279 has the potential to be associated with 14-3-3 (Figure 3. 9A). It is possible that phosphorylation of PEX5 by AMPK at Ser279 is bound by 14-3-3 proteins. Indeed, co-immunoprecipitation assay showed that Myc-PEX5 interacts with HA-14-3-3 β, further confirmed by reverse co-immunoprecipitation (Figure 3. 9B, C). However, in response to glucose starvation, there is no effect on the PEX5 and 14-3-3 interaction that dominate that less TSC2 and ATM peroxisomal distribution is not because of 14-3-3 and PEX5 interaction (Figure 3. 9D). Another possibility is that glucose starvation abolish docking of the cargo-PEX5 complex to the anchoring factor, PEX14, to inhibit cargo protein peroxisomal delivery. In mammals, PEX5 carries cargo proteins to dock at the peroxisomal membrane by PEX14 and subsequent translocation of the proteins to the lumen of the peroxisome. It is possible AMPK phosphorylation PEX5 at Ser297 blocks the cargo-PEX5 complex directing to PEX14 to disrupt cargo protein peroxisomal translocation. Finally, another possibility is that PEX5 recycling is blocked in response to low energy. Ubiquitination plays a vital role in PEX5 shuttling from the lumen of the peroxisome to the cytosol. PEX5 ubiquitined at Cys11 is activated in an ATP-dependent manner by an ubiquitin-activating enzyme (E1)[74]. It is transferred to an ubiquitin-conjugating enzyme (Ubc, E2, PEX4)[114] that- supported by an ubiquitin-protein ligase (E3, PEX2, PEX10, and PEX12). AMPK serves as a key regulator of energy homeostasis by promoting catabolic pathways, resulting in

ATP generation, and inhibition of anabolic pathways that consume ATP. Because ubiquitination is an ATP dependent process, it is possible AMPK phosphorylation of PEX5 at Ser279 inhibits Cys11 ubiquitination to block ATP consuming in response to low energy.

Peroxisomes are cellular organelles that play a central role in lipid metabolism, such as β-oxidation of VLCFAs, and ROS homeostasis. Although the mechanism of peroxisomal matrix proteins, which contribute to several crucial metabolic processes, import is not well characterized, maintaining peroxisome metabolic pathway homeostasis is critical. Deficiency in β-oxidation enzymes, such acyl-CoA oxidase or D-bifunctional protein, causes pathologies known collectively known as PEDs[26]. Overload of redox enzymes, such as D-amino acid oxidase, may cause oxidative damage and promote diseases such as cancer[5]. Together with the data showed in this chapter identified a novel signaling cascade within the peroxisome and a new role for AMPK signaling in the regulation of peroxisomal dynamics.

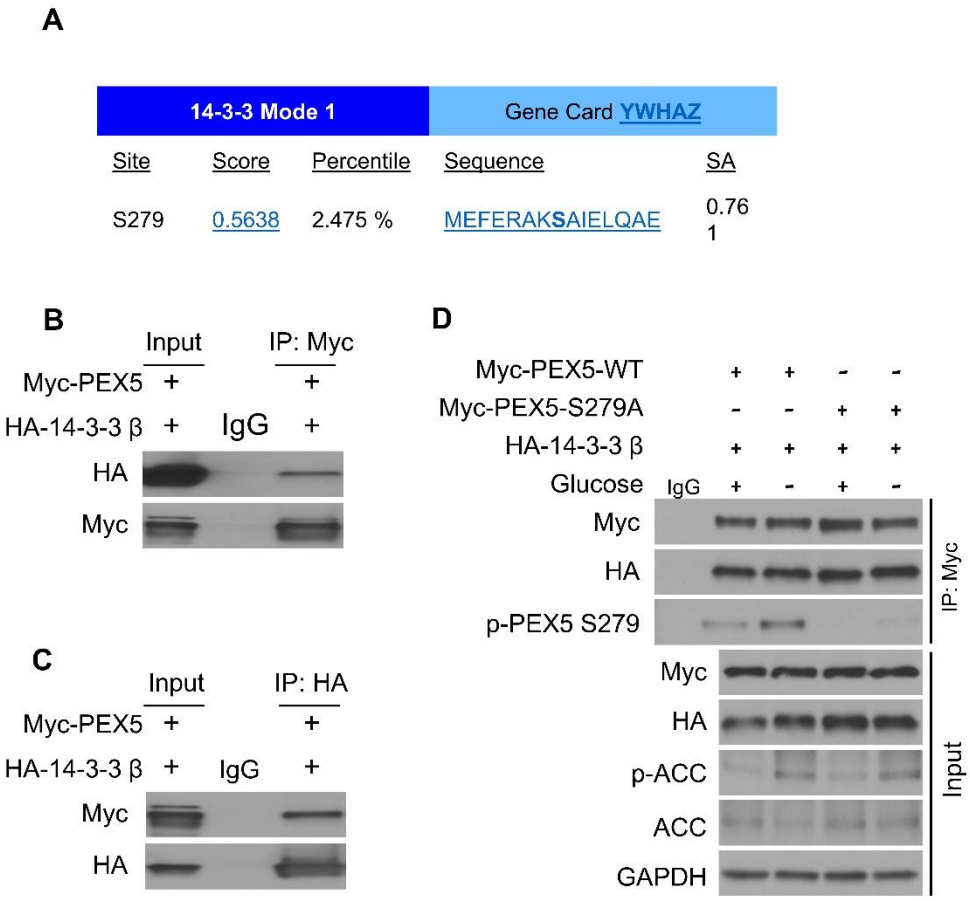

Figure 3. 9 PEX5 phosphorylation at Ser279 is not required for 14-3-3 and PEX5 interaction.

A. Identification of potential 14-3-3 binding sites in PEX5 using Scansite. **B-C.** Myc-PEX5 and HA-14-3-3 β were transfected into HEK293T cells. Cell lysates and Myc/HA pulldowns were immuoblotted as indicated. **D.** HEK293T cells were transfected with Myc-PEX5 WT or Myc-PEX5 S279A for 24 hours. Immunoprecipitation used anti-Myc antibody and blotting with indicated antibodies.

CHAPTER IV

CONCLUSION AND FUTURE DIRECTION

The data presented here have led to two key findings with functional implications for the peroxisomal autophagy and molecular translocation process of PTS1 cargoes by the import receptor PEX5.

In a previous study, our group identified that ATM functions as a signaling kinase in the cytoplasm in response to ROS/RNS that plays an important role in protecting the cell from both DNA and oxidative damage[53,88]. Additional studies showed that the peroxisome is a signaling node involved in the regulation of mTORC1 and autophagy via the TSC tumor suppressor dependent signaling pathway in response to ROS[64]. The data we present in chapter II continued this line of study and found that ATM signaling at the peroxisome participates in pexophagy via two pathways. The first is activation of AMPK and TSC2, leading to repression of mTORC1 in response to ROS. mTORC1 is a well-known inhibitor of autophagy[115], and relief of this repression via AMPK activation and phosphorylation of ULK1 at S317 would increase autophagic flux[116]. The second is phosphorylation of PEX5, which triggers ubiquitination of this peroxisomal receptor protein, binding of the autophagy adapter protein, p62, and targeting peroxisomes to autophagosome for pexophagy. Since ROS can be produced by other organelles, it will be interesting to determine if ROS produced at other sites, such as mitochondria, activates ATM and induces pexophagy, or if

mechanisms exist to prevent peroxisomes from being targeted for pexophagy in response to ROS produced elsewhere in the cell. There are several possible mechanisms by which cells could regulate pexophagy in response to ROS to provide organelle-specificity. For example, when oxidized by ROS, ATM forms an active dimer[117]. We do not know at this time if PEX5 recognizes and binds ATM as a monomer or a dimer, the former of which could provide specificity as an ATM dimer activated elsewhere would not be imported into the peroxisome. Another possibility is that additional modification of ATM at the peroxisome could contribute to specificity. Activation of ATM by RNS also opens up the possibility ATM could be modified (S-nitrosylated) by RNS generated at the peroxisome, which would also potentially contribute to specificity. Whether ROS produced by other organelles can lead to pexophagy and/or ATM-mediated phosphorylation/ubiquitination of PEX5 at the sites we identified (S141 and K209) is also not known. While S141 appears to be necessary for ROS-induced ubiquitination, we do not know if it is sufficient, and perhaps there are other sites/modifications that occur on PEX5 (or other peroxisomal proteins) and contribute to specificity, modifications that could occur only at peroxisomes, or specifically in response to peroxisomal ROS/RNS. In Chapter II, we demonstrated that the phosphomimetic S141E PEX5 mutation alone was unable to induce pexophagy in the absence of ATM activation by ROS (Figure 2. 14) suggests that both mTORC1 repression and PEX5 phosphorylation are important. In Chapter III, the data showed that PEX5 was also phosphorylated at

Ser279 in response to ROS (Figure 3. 4B), indicating another possibility that S279 phosphorylation of PEX5 is also necessary to induce pexophagy in response to ROS. These interesting possibilities need further identifying.
The study we present in Chapter II reveals an important new role for ATM in metabolism as a sensor of ROS that regulates pexophagy. However, many aspects of peroxisome biology involved in peroxisomal biogenesis and cellular metabolism are still undefined.

Mammalian peroxisomes are highly metabolic organelles without its own DNA. All matrix proteins are synthesized in cytosol and transported to peroxisome by import receptors[24]. Deficiency in matrix proteins import, such as β-oxidation enzyme and H_2O_2-degrading enzyme-catalase, causes seriously pathologies known as PBDs and PEDs. Patients with Zellweger syndrome are born with congenital neurological and other abnormalities and usually die within the first year of life. Several defects of peroxisomal protein import systems, among them the PEX5-associated PTS1 pathway, have been found in such patients[118]. In cell lines from Zellweger patients and from PEX5-knockout mice, peroxisomes are absent or grossly deficient and peroxisomal proteins are synthesized but remain localized to the cytoplasm and are subjected to degradation by proteolysis. Although peroxisomal targeting signal and its import receptor are well studied, the mechanism of how the peroxisomal matrix proteins recognition and translocation are still not well characterized. My work, in chapter III, focused on uncovering novel kinases (with focus on AMPK) at the

peroxisome, and found that 1) peroxisome is a signaling organelle involved in the AMPK signaling pathway, 2) AMPK directly phosphorylates PEX5 at Ser279 (Figure 3. 3), and 3) ATM and TSC2, which are localized to the peroxisome by PEX5, peroxisome distribution are decreased in response to low energy (Figure 3. 7), but no effect on the interaction between PEX5 and ATM or TSC2 (Figure 3. 6). Interestingly, the results of present study showed that ATM and TSC2 are less distribution in the peroxisome in response to low energy (Figure 3. 7). In contrast, phospho-ATM and TSC2 were increased in the peroxisome by H_2O_2 (Figure 2. 2 and Figure 4. 1). This suggests the interesting possibility that AMPK phosphorylation of PEX5 at Ser279 may prevent peroxisome from pexophagy, while ATM phosphorylation of PEX5 at Ser141 promotes pexophagy.

Since PEX5 recognizes newly synthesized proteins with the PTS1 motif in the cytosol and promotes their translocation across the peroxisomal membrane, the results of the present study suggest that peroxisomal proteins with PTS1 motif may be synthesized and recognized by import receptor-PEX5 in cytosol but fail to be transported to peroxisomes in response to low energy (Figure 4. 2). The mechanism(s) of preventing PTS1 protein peroxisomal delivery still await further investigation. Possible explanations include 1) 14-3-3 trapping cargo-PEX5 complex in the cytosol; 2) Glucose starvation abolishing cargo-PEX5 complex docking to anchoring factor, PEX14, to inhibit cargo protein peroxisomal delivery (Figure 3. 8).

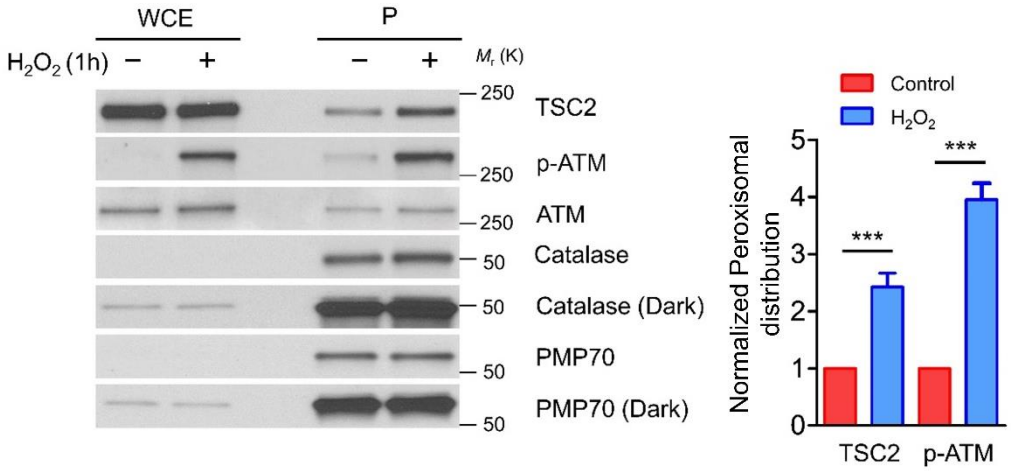

Figure 4. 1 TSC2 and p-ATM peroxisomal distribution in response to ROS.

HEK293T cells treated with H_2O_2 (0.4 mM) for 1 hour. Whole cell extracts (WCE) and peroxisomal fractions (P) were probed with the indicated antibodies. The plot on the right shows the quantification of TSC2 intensities normalized to PMP70 intensities from the peroxisomal fraction.

The reason accounting for the low distribution of ATM and TSC2 in response to low energy is not known. As an energy sensor, AMPK switches on catabolic processes that generate ATP and switches off ATP-consuming pathways. It is possible that AMPK blocks pexophagy and regulates peroxisomal β-oxidation in response to energy stress. Although peroxisomes do not generate ATP directly, it oxidizes fatty acids down to a short chain fatty acids, which are exported to mitochondria for total degradation and to generate ATP in TCA

cycle. Hence, AMPK serves as a “rheostat” that regulates energy homeostasis via peroxisome dynamics and functions in response to low energy.

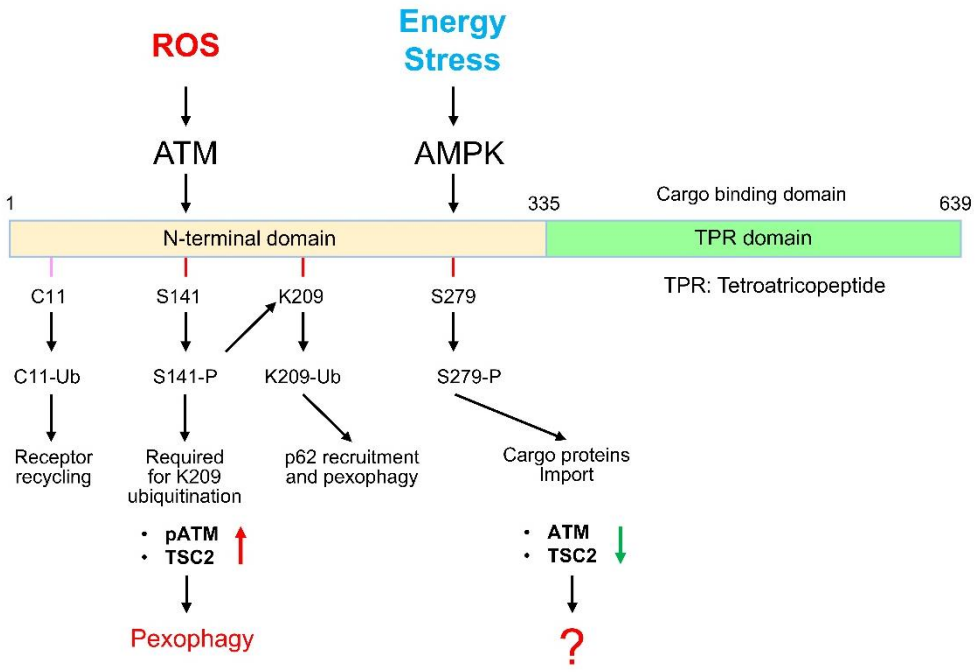

Figure 4. 2 Model for the ATM and AMPK regulation of PEX5 phosphorylation at Ser 141 for peroxisome degradation in response to ROS; at Ser 279 for peroxisomal cargo proteins import in response to low energy.

Furthermore, peroxisomal enzymes contribute to several crucial metabolic processes, such as β-oxidation of VLCFAs and metabolism of ROS/RNS. Maintain redox metabolic homeostasis is critical for normal function of

peroxisome. Excess ROS can cause cellular damage and link to over 150 diseases such as cancer[5]. Thus elucidating key cell signaling pathways that regulate redox metabolic enzyme transport is important for redox homeostasis. Interestingly, the results of present study showed that some PTS1 proteins are less distribution in the peroxisome in response to low energy. This suggests the interesting possibility that AMPK phosphorylation of PEX5 at Ser279 may prevent H_2O_2-producing oxidase, such as D-amino acid oxidase (DAO) and Acyl-CoA oxidase (ACOX), peroxisomal distribution, reducing H_2O_2 production. This represents a novel mechanism to prevent excessive production of ROS in peroxisomes. Moreover, a future challenge remains in the determination of the events leading to cargo-receptor docking to the peroxisomal membrane, releasing proteins into the lumen of peroxisomes and receptor recycling. Further, it will be of specific interest to investigate the functional implications of potential factors or regulators during the peroxisomal proteins translocation cycle. These (and other) possibilities now await further exploration.

Our previous studies and the data described in this dissertation provide two models (Figure 2. 16 and Figure 4. 2) to investigate peroxisome dynamics in response to different stress. ROS-induced ATM signals to the TSC-mTORC1, PEX5 phosphorylation, ubiquitination and recognition of Ub-PEX5 by p62 to trigger peroxisome degradation. This model led us to reason that ROS acts as a “rheostat” for peroxisomal homeostasis. Moreover AMPK, a major metabolic regulator, phosphorylates import receptor PEX5 to regulate peroxisomal proteins

delivery in response to low energy. These new concepts uncover crucial roles for the ATM and AMPK signaling pathway at the peroxisome and open new horizons for understanding peroxisomal homeostasis and its role in cellular metabolism. The inability to maintain peroxisome homeostasis would result in accumulation of damaged/dysfunctional peroxisomes, redox disequilibrium, and increased cancer risk[5]. Abnormal delivery of peroxisomal matrix proteins would disrupt several anabolic and catabolic reactions that promote peroxisomal enzyme deficiency disorders[119]. Thus, the function of ATM and AMPK as signaling kinases at the peroxisome in response to ROS/low energy may be key factors for monitoring peroxisome homeostasis and functions.

REFERENCES

1 Schrader, M. Shared components of mitochondrial and peroxisomal division. *Biochimica et biophysica acta* **1763**, 531-541, doi:10.1016/j.bbamcr.2006.01.004 (2006).

2 Rhodin, J. A. G. *Correlation of ultrastructural organization and function in normal and experimentally chaged proximal convoluted tubule cells of the mouse kidney*. (1954).

3 Tolbert, N. E. & Essner, E. Microbodies: peroxisomes and glyoxysomes. *The Journal of cell biology* **91**, 271s-283s (1981).

4 De Duve, C. & Baudhuin, P. Peroxisomes (microbodies and related particles). *Physiological reviews* **46**, 323-357, doi:10.1152/physrev.1966.46.2.323 (1966).

5 Fransen, M., Nordgren, M., Wang, B. & Apanasets, O. Role of peroxisomes in ROS/RNS-metabolism: implications for human disease. *Biochimica et biophysica acta* **1822**, 1363-1373, doi:10.1016/j.bbadis.2011.12.001 (2012).

6 van den Bosch, H., Schutgens, R. B., Wanders, R. J. & Tager, J. M. Biochemistry of peroxisomes. *Annual review of biochemistry* **61**, 157-197, doi:10.1146/annurev.bi.61.070192.001105 (1992).

7 Mannaerts, G. P. & Van Veldhoven, P. P. Role of peroxisomes in mammalian metabolism. *Cell biochemistry and function* **10**, 141-151, doi:10.1002/cbf.290100303 (1992).

8 Douce, R., Bourguignon, J., Neuburger, M. & Rebeille, F. The glycine decarboxylase system: a fascinating complex. *Trends in plant science* **6**, 167-176 (2001).

9 Hayashi, M. & Nishimura, M. Entering a new era of research on plant peroxisomes. *Current opinion in plant biology* **6**, 577-582 (2003).

10 Goepfert, S. & Poirier, Y. Beta-oxidation in fatty acid degradation and beyond. *Current opinion in plant biology* **10**, 245-251, doi:10.1016/j.pbi.2007.04.007 (2007).

11 Schrader, M., Costello, J., Godinho, L. F. & Islinger, M. Peroxisome-mitochondria interplay and disease. *Journal of inherited metabolic disease* **38**, 681-702, doi:10.1007/s10545-015-9819-7 (2015).

12 Schrader, M. & Yoon, Y. Mitochondria and peroxisomes: are the 'big brother' and the 'little sister' closer than assumed? *BioEssays : news and reviews in molecular, cellular and developmental biology* **29**, 1105-1114, doi:10.1002/bies.20659 (2007).

13 Eckert, J. H. & Erdmann, R. Peroxisome biogenesis. *Reviews of physiology, biochemistry and pharmacology* **147**, 75-121, doi:10.1007/s10254-003-0007-z (2003).

14 Ma, C., Agrawal, G. & Subramani, S. Peroxisome assembly: matrix and membrane protein biogenesis. *The Journal of cell biology* **193**, 7-16, doi:10.1083/jcb.201010022 (2011).

15 Gould, S. J., Keller, G. A., Hosken, N., Wilkinson, J. & Subramani, S. A conserved tripeptide sorts proteins to peroxisomes. *The Journal of cell biology* **108**, 1657-1664 (1989).

16 Brocard, C. & Hartig, A. Peroxisome targeting signal 1: is it really a simple tripeptide? *Biochimica et biophysica acta* **1763**, 1565-1573, doi:10.1016/j.bbamcr.2006.08.022 (2006).

17 Swinkels, B. W., Gould, S. J., Bodnar, A. G., Rachubinski, R. A. & Subramani, S. A novel, cleavable peroxisomal targeting signal at the amino-terminus of the rat 3-ketoacyl-CoA thiolase. *The EMBO journal* **10**, 3255-3262 (1991).

18 Lazarow, P. B. The import receptor Pex7p and the PTS2 targeting sequence. *Biochimica et biophysica acta* **1763**, 1599-1604, doi:10.1016/j.bbamcr.2006.08.011 (2006).

19 Stanley, W. A. *et al.* Recognition of a functional peroxisome type 1 target by the dynamic import receptor pex5p. *Molecular cell* **24**, 653-663, doi:10.1016/j.molcel.2006.10.024 (2006).

20 Rayapuram, N. & Subramani, S. The importomer--a peroxisomal membrane complex involved in protein translocation into the peroxisome

matrix. *Biochimica et biophysica acta* **1763**, 1613-1619, doi:10.1016/j.bbamcr.2006.08.035 (2006).

21 Saveria, T. *et al.* Conservation of PEX19-binding motifs required for protein targeting to mammalian peroxisomal and trypanosome glycosomal membranes. *Eukaryotic cell* **6**, 1439-1449, doi:10.1128/EC.00084-07 (2007).

22 Dimitrov, L., Lam, S. K. & Schekman, R. The role of the endoplasmic reticulum in peroxisome biogenesis. *Cold Spring Harbor perspectives in biology* **5**, a013243, doi:10.1101/cshperspect.a013243 (2013).

23 Smith, J. J. & Aitchison, J. D. Peroxisomes take shape. *Nature reviews. Molecular cell biology* **14**, 803-817, doi:10.1038/nrm3700 (2013).

24 Lazarow, P. B. & Fujiki, Y. Biogenesis of peroxisomes. *Annual review of cell biology* **1**, 489-530, doi:10.1146/annurev.cb.01.110185.002421 (1985).

25 Koch, A. *et al.* Dynamin-like protein 1 is involved in peroxisomal fission. *The Journal of biological chemistry* **278**, 8597-8605, doi:10.1074/jbc.M211761200 (2003).

26 Wanders, R. J. & Waterham, H. R. Peroxisomal disorders: the single peroxisomal enzyme deficiencies. *Biochimica et biophysica acta* **1763**, 1707-1720, doi:10.1016/j.bbamcr.2006.08.010 (2006).

27 Wanders, R. J. Peroxisomes, lipid metabolism, and peroxisomal disorders. *Molecular genetics and metabolism* **83**, 16-27, doi:10.1016/j.ymgme.2004.08.016 (2004).

28 Fransen, M., Nordgren, M., Wang, B., Apanasets, O. & Van Veldhoven, P. P. Aging, age-related diseases and peroxisomes. *Sub-cellular biochemistry* **69**, 45-65, doi:10.1007/978-94-007-6889-5_3 (2013).

29 Kliewer, S. A., Umesono, K., Noonan, D. J., Heyman, R. A. & Evans, R. M. Convergence of 9-cis retinoic acid and peroxisome proliferator signalling pathways through heterodimer formation of their receptors. *Nature* **358**, 771-774, doi:10.1038/358771a0 (1992).

30 Meng, T. C., Fukada, T. & Tonks, N. K. Reversible oxidation and inactivation of protein tyrosine phosphatases in vivo. *Molecular cell* **9**, 387-399 (2002).

31 Reddy, J. K. & Hashimoto, T. Peroxisomal beta-oxidation and peroxisome proliferator-activated receptor alpha: an adaptive metabolic system. *Annual review of nutrition* **21**, 193-230, doi:10.1146/annurev.nutr.21.1.193 (2001).

32 Schrader, M. & Fahimi, H. D. Peroxisomes and oxidative stress. *Biochim Biophys Acta* **1763**, 1755-1766, doi:10.1016/j.bbamcr.2006.09.006 (2006).

33 Holmstrom, K. M. & Finkel, T. Cellular mechanisms and physiological consequences of redox-dependent signalling. *Nature reviews. Molecular cell biology* **15**, 411-421, doi:10.1038/nrm3801 (2014).

34 Alexander, A. *et al.* ATM signals to TSC2 in the cytoplasm to regulate mTORC1 in response to ROS. *Proc Natl Acad Sci U S A* **107**, 4153-4158, doi:10.1073/pnas.0913860107 (2010).

35 Chen, Y., Azad, M. B. & Gibson, S. B. Superoxide is the major reactive oxygen species regulating autophagy. *Cell Death Differ* **16**, 1040-1052, doi:10.1038/cdd.2009.49 (2009).

36 Scherz-Shouval, R. *et al.* Reactive oxygen species are essential for autophagy and specifically regulate the activity of Atg4. *Embo J* **26**, 1749-1760, doi:10.1038/sj.emboj.7601623 (2007).

37 Purdue, P. E. & Lazarow, P. B. Peroxisome biogenesis. *Annu Rev Cell Dev Biol* **17**, 701-752, doi:10.1146/annurev.cellbio.17.1.701 (2001).

38 Santos, M. J. *et al.* Peroxisomal proliferation protects from beta-amyloid neurodegeneration. *The Journal of biological chemistry* **280**, 41057-41068, doi:10.1074/jbc.M505160200 (2005).

39 Singh, I., Singh, A. K. & Contreras, M. A. Peroxisomal dysfunction in inflammatory childhood white matter disorders: an unexpected contributor to neuropathology. *Journal of child neurology* **24**, 1147-1157, doi:10.1177/0883073809338327 (2009).

40 Weller, S., Gould, S. J. & Valle, D. Peroxisome biogenesis disorders. *Annu Rev Genomics Hum Genet* **4**, 165-211, doi:10.1146/annurev.genom.4.070802.110424 (2003).

41 Reuber, B. E. *et al.* Mutations in PEX1 are the most common cause of peroxisome biogenesis disorders. *Nature genetics* **17**, 445-448, doi:10.1038/ng1297-445 (1997).

42 Dunn, W. A., Jr. *et al.* Pexophagy: the selective autophagy of peroxisomes. *Autophagy* **1**, 75-83 (2005).

43 Farre, J. C. & Subramani, S. Peroxisome turnover by micropexophagy: an autophagy-related process. *Trends Cell Biol* **14**, 515-523, doi:10.1016/j.tcb.2004.07.014 (2004).

44 Iwata, J. *et al.* Excess peroxisomes are degraded by autophagic machinery in mammals. *The Journal of biological chemistry* **281**, 4035-4041, doi:10.1074/jbc.M512283200 (2006).

45 Klionsky, D. J. *et al.* Guidelines for the use and interpretation of assays for monitoring autophagy. *Autophagy* **8**, 445-544 (2012).

46 Till, A., Lakhani, R., Burnett, S. F. & Subramani, S. Pexophagy: the selective degradation of peroxisomes. *International journal of cell biology* **2012**, 512721, doi:10.1155/2012/512721 (2012).

47 Kirkin, V., McEwan, D. G., Novak, I. & Dikic, I. A role for ubiquitin in selective autophagy. *Molecular cell* **34**, 259-269, doi:10.1016/j.molcel.2009.04.026 (2009).

48 Deosaran, E. *et al.* NBR1 acts as an autophagy receptor for peroxisomes. *Journal of cell science* **126**, 939-952, doi:10.1242/jcs.114819 (2013).

49 Kim, P. K., Hailey, D. W., Mullen, R. T. & Lippincott-Schwartz, J. Ubiquitin signals autophagic degradation of cytosolic proteins and peroxisomes. *Proc Natl Acad Sci U S A* **105**, 20567-20574, doi:10.1073/pnas.0810611105 (2008).

50 Kastan, M. B. & Bartek, J. Cell-cycle checkpoints and cancer. *Nature* **432**, 316-323, doi:10.1038/nature03097 (2004).

51 Schneider, J. G. *et al.* ATM-dependent suppression of stress signaling reduces vascular disease in metabolic syndrome. *Cell metabolism* **4**, 377-389, doi:10.1016/j.cmet.2006.10.002 (2006).

52 Matsuoka, S. *et al.* ATM and ATR substrate analysis reveals extensive protein networks responsive to DNA damage. *Science* **316**, 1160-1166, doi:10.1126/science.1140321 (2007).

53 Alexander, A. *et al.* ATM signals to TSC2 in the cytoplasm to regulate mTORC1 in response to ROS. *Proceedings of the National Academy of Sciences of the United States of America* **107**, 4153-4158, doi:10.1073/pnas.0913860107 (2010).

54 Aspuria, P. J. & Tamanoi, F. The Rheb family of GTP-binding proteins. *Cell Signal* **16**, 1105-1112, doi:10.1016/j.cellsig.2004.03.019 (2004).

55 Huang, J. & Manning, B. D. The TSC1-TSC2 complex: a molecular switchboard controlling cell growth. *Biochem J* **412**, 179-190, doi:10.1042/BJ20080281 (2008).

56 Crino, P. B., Nathanson, K. L. & Henske, E. P. The tuberous sclerosis complex. *N Engl J Med* **355**, 1345-1356, doi:10.1056/NEJMra055323 (2006).

57 Wullschleger, S., Loewith, R. & Hall, M. N. TOR signaling in growth and metabolism. *Cell* **124**, 471-484, doi:10.1016/j.cell.2006.01.016 (2006).

58 Inoki, K., Corradetti, M. N. & Guan, K. L. Dysregulation of the TSC-mTOR pathway in human disease. *Nature genetics* **37**, 19-24, doi:10.1038/ng1494 (2005).

59 He, C. & Klionsky, D. J. Regulation mechanisms and signaling pathways of autophagy. *Annu Rev Genet* **43**, 67-93, doi:10.1146/annurev-genet-102808-114910 (2009).

60 Hosokawa, N. *et al.* Nutrient-dependent mTORC1 association with the ULK1-Atg13-FIP200 complex required for autophagy. *Mol Biol Cell* **20**, 1981-1991, doi:10.1091/mbc.E08-12-1248 (2009).

61 Jung, C. H. *et al.* ULK-Atg13-FIP200 complexes mediate mTOR signaling to the autophagy machinery. *Mol Biol Cell* **20**, 1992-2003, doi:10.1091/mbc.E08-12-1249 (2009).

62 Kim, J., Kundu, M., Viollet, B. & Guan, K. L. AMPK and mTOR regulate autophagy through direct phosphorylation of Ulk1. *Nature cell biology* **13**, 132-141, doi:10.1038/ncb2152 (2011).

63 Mizushima, N., Yoshimori, T. & Levine, B. Methods in mammalian autophagy research. *Cell* **140**, 313-326, doi:10.1016/j.cell.2010.01.028 (2010).

64 Zhang, J. *et al.* A tuberous sclerosis complex signalling node at the peroxisome regulates mTORC1 and autophagy in response to ROS. *Nature cell biology* **15**, 1186-1196, doi:10.1038/ncb2822 (2013).

65 Kastan, M. B. & Lim, D. S. The many substrates and functions of ATM. *Nature reviews. Molecular cell biology* **1**, 179-186, doi:10.1038/35043058 (2000).

66 Lim, D. S. *et al.* ATM binds to beta-adaptin in cytoplasmic vesicles. *Proc Natl Acad Sci U S A* **95**, 10146-10151 (1998).

67 Watters, D. *et al.* Localization of a portion of extranuclear ATM to peroxisomes. *The Journal of biological chemistry* **274**, 34277-34282 (1999).

68 Fu, Y. N. *et al.* Metformin attenuates pressure overload-induced cardiac hypertrophy via AMPK activation. *Acta pharmacologica Sinica* **32**, 879-887, doi:10.1038/aps.2010.229 (2011).

69 Kim, S. T., Lim, D. S., Canman, C. E. & Kastan, M. B. Substrate specificities and identification of putative substrates of ATM kinase family members. *The Journal of biological chemistry* **274**, 37538-37543 (1999).

70 Stryer, L. *Biochemistry*. 4. edn, (W.H. Freeman, 1995).

71 Mann, M. *et al.* Analysis of protein phosphorylation using mass spectrometry: deciphering the phosphoproteome. *Trends in biotechnology* **20**, 261-268 (2002).

72 Kim, P. K., Hailey, D. W., Mullen, R. T. & Lippincott-Schwartz, J. Ubiquitin signals autophagic degradation of cytosolic proteins and peroxisomes. *Proceedings of the National Academy of Sciences of the United States of America* **105**, 20567-20574, doi:10.1073/pnas.0810611105 (2008).

73 Brown, A. I., Kim, P. K. & Rutenberg, A. D. PEX5 and ubiquitin dynamics on mammalian peroxisome membranes. *PLoS computational biology* **10**, e1003426, doi:10.1371/journal.pcbi.1003426 (2014).

74 Carvalho, A. F. *et al.* Ubiquitination of mammalian Pex5p, the peroxisomal import receptor. *The Journal of biological chemistry* **282**, 31267-31272, doi:10.1074/jbc.M706325200 (2007).

75 Grou, C. P. *et al.* Members of the E2D (UbcH5) family mediate the ubiquitination of the conserved cysteine of Pex5p, the peroxisomal import receptor. *The Journal of biological chemistry* **283**, 14190-14197, doi:10.1074/jbc.M800402200 (2008).

76 Platta, H. W. *et al.* Pex2 and pex12 function as protein-ubiquitin ligases in peroxisomal protein import. *Molecular and cellular biology* **29**, 5505-5516, doi:10.1128/MCB.00388-09 (2009).

77 Thoms, S. & Erdmann, R. Peroxisomal matrix protein receptor ubiquitination and recycling. *Biochim Biophys Acta* **1763**, 1620-1628, doi:10.1016/j.bbamcr.2006.08.046 (2006).

78 Platta, H. W., Girzalsky, W. & Erdmann, R. Ubiquitination of the peroxisomal import receptor Pex5p. *The Biochemical journal* **384**, 37-45, doi:10.1042/BJ20040572 (2004).

79 Wagner, S. A. *et al.* A proteome-wide, quantitative survey of in vivo ubiquitylation sites reveals widespread regulatory roles. *Molecular &*

cellular proteomics : MCP **10**, M111 013284, doi:10.1074/mcp.M111.013284 (2011).

80 Hunter, T. The age of crosstalk: phosphorylation, ubiquitination, and beyond. *Molecular cell* **28**, 730-738, doi:10.1016/j.molcel.2007.11.019 (2007).

81 Nazarko, T. Y. *et al.* Peroxisomal Atg37 binds Atg30 or palmitoyl-CoA to regulate phagophore formation during pexophagy. *J Cell Biol* **204**, 541-557, doi:10.1083/jcb.201307050 (2014).

82 Chen, Y. & Dorn, G. W., 2nd. PINK1-phosphorylated mitofusin 2 is a Parkin receptor for culling damaged mitochondria. *Science* **340**, 471-475, doi:10.1126/science.1231031 (2013).

83 Geisler, S. *et al.* PINK1/Parkin-mediated mitophagy is dependent on VDAC1 and p62/SQSTM1. *Nat Cell Biol* **12**, 119-131, doi:10.1038/ncb2012 (2010).

84 Shiba-Fukushima, K. *et al.* PINK1-mediated phosphorylation of the Parkin ubiquitin-like domain primes mitochondrial translocation of Parkin and regulates mitophagy. *Scientific reports* **2**, 1002, doi:10.1038/srep01002 (2012).

85 Zhang, J. *et al.* ATM functions at the peroxisome to induce pexophagy in response to ROS. *Nature cell biology* **17**, 1259-1269, doi:10.1038/ncb3230 (2015).

86 Hara-Kuge, S. & Fujiki, Y. The peroxin Pex14p is involved in LC3-dependent degradation of mammalian peroxisomes. *Experimental cell research* **314**, 3531-3541, doi:10.1016/j.yexcr.2008.09.015 (2008).

87 Otera, H. *et al.* Peroxisomal targeting signal receptor Pex5p interacts with cargoes and import machinery components in a spatiotemporally differentiated manner: conserved Pex5p WXXXF/Y motifs are critical for matrix protein import. *Molecular and cellular biology* **22**, 1639-1655 (2002).

88 Tripathi, D. N. *et al.* Reactive nitrogen species regulate autophagy through ATM-AMPK-TSC2-mediated suppression of mTORC1. *Proceedings of the National Academy of Sciences of the United States of America* **110**, E2950-2957, doi:10.1073/pnas.1307736110 (2013).

89 Walton, P. A. Import of stably-folded proteins into peroxisomes. *Annals of the New York Academy of Sciences* **804**, 76-85 (1996).

90 Braverman, N., Dodt, G., Gould, S. J. & Valle, D. An isoform of pex5p, the human PTS1 receptor, is required for the import of PTS2 proteins into peroxisomes. *Human molecular genetics* **7**, 1195-1205 (1998).

91 Hettema, E. H., Girzalsky, W., van Den Berg, M., Erdmann, R. & Distel, B. Saccharomyces cerevisiae pex3p and pex19p are required for proper localization and stability of peroxisomal membrane proteins. *The EMBO journal* **19**, 223-233, doi:10.1093/emboj/19.2.223 (2000).

92 Elsasser, S. & Finley, D. Delivery of ubiquitinated substrates to protein-unfolding machines. *Nature cell biology* **7**, 742-749, doi:10.1038/ncb0805-742 (2005).

93 Gatto, G. J., Jr., Geisbrecht, B. V., Gould, S. J. & Berg, J. M. Peroxisomal targeting signal-1 recognition by the TPR domains of human PEX5. *Nature structural biology* **7**, 1091-1095, doi:10.1038/81930 (2000).

94 Saidowsky, J. *et al.* The di-aromatic pentapeptide repeats of the human peroxisome import receptor PEX5 are separate high affinity binding sites for the peroxisomal membrane protein PEX14. *The Journal of biological chemistry* **276**, 34524-34529, doi:10.1074/jbc.M104647200 (2001).

95 Faber, K. N., Heyman, J. A. & Subramani, S. Two AAA family peroxins, PpPex1p and PpPex6p, interact with each other in an ATP-dependent manner and are associated with different subcellular membranous structures distinct from peroxisomes. *Molecular and cellular biology* **18**, 936-943 (1998).

96 Carling, D., Thornton, C., Woods, A. & Sanders, M. J. AMP-activated protein kinase: new regulation, new roles? *The Biochemical journal* **445**, 11-27, doi:10.1042/BJ20120546 (2012).

97 Oakhill, J. S., Scott, J. W. & Kemp, B. E. AMPK functions as an adenylate charge-regulated protein kinase. *Trends in endocrinology and metabolism: TEM* **23**, 125-132, doi:10.1016/j.tem.2011.12.006 (2012).

98 Hawley, S. A. *et al.* Characterization of the AMP-activated protein kinase kinase from rat liver and identification of threonine 172 as the major site at which it phosphorylates AMP-activated protein kinase. *The Journal of biological chemistry* **271**, 27879-27887 (1996).

99 Gowans, G. J., Hawley, S. A., Ross, F. A. & Hardie, D. G. AMP is a true physiological regulator of AMP-activated protein kinase by both allosteric activation and enhancing net phosphorylation. *Cell metabolism* **18**, 556-566, doi:10.1016/j.cmet.2013.08.019 (2013).

100 Xiao, B. *et al.* Structure of mammalian AMPK and its regulation by ADP. *Nature* **472**, 230-233, doi:10.1038/nature09932 (2011).

101 Carretero, J. *et al.* Dysfunctional AMPK activity, signalling through mTOR and survival in response to energetic stress in LKB1-deficient lung cancer. *Oncogene* **26**, 1616-1625, doi:10.1038/sj.onc.1209951 (2007).

102 Fogarty, S. *et al.* Calmodulin-dependent protein kinase kinase-beta activates AMPK without forming a stable complex: synergistic effects of Ca2+ and AMP. *The Biochemical journal* **426**, 109-118, doi:10.1042/BJ20091372 (2010).

103 Hardie, D. G., Ross, F. A. & Hawley, S. A. AMPK: a nutrient and energy sensor that maintains energy homeostasis. *Nature reviews. Molecular cell biology* **13**, 251-262, doi:10.1038/nrm3311 (2012).

104 Hardie, D. G. AMP-activated/SNF1 protein kinases: conserved guardians of cellular energy. *Nature reviews. Molecular cell biology* **8**, 774-785, doi:10.1038/nrm2249 (2007).

105 Kim, Y., Roh, S., Lawler, S. & Friedman, A. miR451 and AMPK mutual antagonism in glioma cell migration and proliferation: a mathematical model. *PloS one* **6**, e28293, doi:10.1371/journal.pone.0028293 (2011).

106 Egan, D. F. *et al.* Phosphorylation of ULK1 (hATG1) by AMP-activated protein kinase connects energy sensing to mitophagy. *Science* **331**, 456-461, doi:10.1126/science.1196371 (2011).

107 Kim, J. *et al.* Differential regulation of distinct Vps34 complexes by AMPK in nutrient stress and autophagy. *Cell* **152**, 290-303, doi:10.1016/j.cell.2012.12.016 (2013).

108 Jeon, S. M. Regulation and function of AMPK in physiology and diseases. *Experimental & molecular medicine* **48**, e245, doi:10.1038/emm.2016.81 (2016).

109 Gwinn, D. M. *et al.* AMPK phosphorylation of raptor mediates a metabolic checkpoint. *Molecular cell* **30**, 214-226, doi:10.1016/j.molcel.2008.03.003 (2008).

110 Hardie, D. G., Schaffer, B. E. & Brunet, A. AMPK: An Energy-Sensing Pathway with Multiple Inputs and Outputs. *Trends in cell biology* **26**, 190-201, doi:10.1016/j.tcb.2015.10.013 (2016).

111 Francisco, T. *et al.* A cargo-centered perspective on the PEX5 receptor-mediated peroxisomal protein import pathway. *The Journal of biological chemistry* **288**, 29151-29159, doi:10.1074/jbc.M113.487140 (2013).

112 Hagan, C. R., Daniel, A. R., Dressing, G. E. & Lange, C. A. Role of phosphorylation in progesterone receptor signaling and specificity. *Molecular and cellular endocrinology* **357**, 43-49, doi:10.1016/j.mce.2011.09.017 (2012).

113 Kleppe, R., Martinez, A., Doskeland, S. O. & Haavik, J. The 14-3-3 proteins in regulation of cellular metabolism. *Seminars in cell & developmental biology* **22**, 713-719, doi:10.1016/j.semcdb.2011.08.008 (2011).

114 van der Klei, I. J. *et al.* The ubiquitin-conjugating enzyme Pex4p of Hansenula polymorpha is required for efficient functioning of the PTS1 import machinery. *The EMBO journal* **17**, 3608-3618, doi:10.1093/emboj/17.13.3608 (1998).

115 Jung, C. H., Ro, S. H., Cao, J., Otto, N. M. & Kim, D. H. mTOR regulation of autophagy. *FEBS letters* **584**, 1287-1295, doi:10.1016/j.febslet.2010.01.017 (2010).

116 Kim, J., Kundu, M., Viollet, B. & Guan, K. L. AMPK and mTOR regulate autophagy through direct phosphorylation of Ulk1. *Nature cell biology* **13**, 132-141, doi:10.1038/ncb2152 (2011).

117 Guo, Z., Kozlov, S., Lavin, M. F., Person, M. D. & Paull, T. T. ATM activation by oxidative stress. *Science* **330**, 517-521, doi:10.1126/science.1192912 (2010).

118 Ebberink, M. S. *et al.* Genotype-phenotype correlation in PEX5-deficient peroxisome biogenesis defective cell lines. *Human mutation* **30**, 93-98, doi:10.1002/humu.20833 (2009).

119 Aubourg, P. & Wanders, R. Peroxisomal disorders. *Handbook of clinical neurology* **113**, 1593-1609, doi:10.1016/B978-0-444-59565-2.00028-9 (2013).